

# Yi Zhu

Department of Civil and Environmental Engineering, University of Michigan, Ann Arbor, MI 48109 e-mail: yizhucee@umich.edu

## Mark Schenk

Department of Aerospace Engineering, University of Bristol, Bristol BS8 1TR, UK e-mail: m.schenk@bristol.ac.uk

# Evgueni T. Filipov

Department of Civil and Environmental
Engineering,
University of Michigan,
Ann Arbor, MI 48109;
Department of Mechanical Engineering,
University of Michigan,
Ann Arbor, MI 48109
e-mail: filipov@umich.edu

# A Review on Origami Simulations: From Kinematics, To Mechanics, Toward Multiphysics

Origami-inspired systems are attractive for creating structures and devices with tunable properties, multiple functionalities, high-ratio packaging capabilities, easy fabrication, and many other advantageous properties. Over the past decades, the community has developed a variety of simulation techniques to analyze the kinematic motions, mechanical properties, and multiphysics characteristics of origami systems. These various simulation techniques are formulated with different assumptions and are often tailored to specific origami designs. Thus, it is valuable to systematically review the state-of-the-art in origami simulation techniques. This review presents the formulations of different origami simulations, discusses their strengths and weaknesses, and identifies the potential application scenarios of different simulation techniques. The material presented in this work aims to help origami researchers better appreciate the formulations and underlying assumptions within different origami simulation techniques, and thereby enable the selection and development of appropriate origami simulations. Finally, we look ahead at future challenges in the field of origami simulation. [DOI: 10.1115/1.4055031]

Keywords: origami, kinematic simulation, mechanical simulation, multiphysics simulation

# 1 Introduction, History, and Organization

Folding has generated numerous inspiring phenomena in nature and our daily lives; for example, some insects have wings that include folded edges to help resist loads during flight [1] and proteins require accurately folded three-dimensional (3D) configurations to function properly [2]. Origami artists have long been fascinated by the rich geometries obtained from repeatedly and strategically folding sheets of paper. Inspired by these origami artists, researchers and engineers have explored the potential of building structures and mechanisms with origami principles over the past decades. For example, origami has been used to create metamaterials [3–10], robotic systems [11–18], active microdevices [19-22], biomedical tools [23-27], deployable building structures [28–31], reconfigurable space structures [32–34], packaging systems for engineering devices [35-37], and more [38-43]. Recent review articles have summarized developments in origami including applications in micro- and nanoscale systems [44], architected materials [45], biomedical applications [46], origami robots [47], designs and applications of engineering origami [48], architectural applications [49], and mathematical approaches for design and kinematic folding [50].

Alongside developments in origami designs and applications, many dedicated *simulation techniques* have been developed to analyze the kinematics, mechanics, and multiphysics properties of these thin sheet systems. Simulating the physical behavior of origami forms the basis for understanding, analyzing, designing, and optimizing origami-inspired systems. In light of this, we believe that it is beneficial to review the simulation of origami to categorize different simulation techniques, to summarize the underlying mathematical models and solution methods involved, and to present the strengths and weaknesses of different techniques. Although origami simulation borrows widely from analyses and techniques in other disciplines in science and engineering, there are unique challenges; for example, the pattern geometry and

select and develop appropriate simulation techniques for specific projects. Moreover, because different simulation techniques were developed to answer different questions regarding origami systems, learning about the underlying principles for simulation techniques can also help origami researchers to ask the right questions.

Figure 1 depicts the history of origami simulations in broad brush strokes. Of course, no histories are complete and technical developments are not necessarily sequential; moreover, related simulations can be found in advance of the specific development related to origami. The simulation of origami starts with the analysis of their kinematics, dating back to the early 1970s. The pioneering works by Huffman [51] and by Resch [52] demonstrate

such early efforts to simulate origami folding in a virtual environ-

localized crease behavior can significantly impact the global response, and efficient simulations require careful consideration

of the degrees-of-freedom of the origami system. The presented

material aims to help future origami scientists and engineers to

ment. In the 1990s and 2000s, a number of studies proposed approaches and concepts to simulate the kinematic folding motions of origami [53-57]. These studies pinned down many fundamental ideas for the kinematic simulation techniques of origami. During this period, there were also early works studying the mechanical behavior of origami [58,59]. Starting around 2010, researchers began exploring origami for creating mechanical metamaterials, crash boxes, and other engineering structures [4,5,60]. To capture the mechanical properties of origami systems for these application scenarios, various mechanics-based simulation techniques were created [61-63]. More recently, researchers have started exploring active origami systems that can fold autonomously in response to environmental stimuli and can generate unique nonmechanical behaviors [19,21,24]. In response to the need for capturing the folding behaviors and the nonmechanical properties of active origami systems, researchers have started building multiphysics-based simulation platforms to capture advanced behaviors of origami systems [39,64,65].

The history of origami simulation also gives us a rationale for separating the simulation techniques into three major groups:

kinematics-based simulations, mechanics-based simulations, and multiphysics simulations. These three groups form the three major sections of this review; within each section, we will categorize the simulations based on their formulation rather than their chronological order. First, we will briefly discuss the scope of this work and the terminology, before expanding on each of the three identified categories. Following these three sections, we will summarize existing simulation packages, discuss how to select appropriate simulation techniques, and discuss future challenges in the field.

## 2 Scope and Terminology

This section outlines the scope of the paper and introduces important terminologies related to origami simulations. The focus of this work is the simulation of origami systems, which answers the question of how to simulate the folding motions and the corresponding property changes in origami systems. This paper will therefore not focus on the design of origami systems, which includes problems such as how to generate new origami patterns, solve mountain-valley assignments, and adjust existing patterns for certain applications. Nonetheless, we expect that this paper will provide useful information for origami designers to select and build suitable simulation techniques for their specific problems.

Moreover, we will focus on the simulation of origami with straight creases. Simulating the behavior of curved creases often requires drastically different formulations [66]. For example, defining a straight crease only requires specifying two nodes at the end of the crease and the folding can be represented with a single scalar variable. In contrast, defining a curve crease requires using mathematical tools such as spline or polynomial functions, and the fold angle can vary along the length of the crease. The simulation techniques covered in this review will also be applicable to the analysis of a wide range of kirigami systems, where cuts are introduced, provided that the folding creases remain straight.

**2.1 Model, Solution Method, Simulation.** Before introducing specific origami terminologies, we first discuss three fundamental terms used in the simulation of physical systems: *model, solution method,* and *simulation*. In many situations, these three terms are used interchangeably; however, we believe it is best to define and use these terms more carefully.

*Model:* In this work, we define a model as a mathematical representation of physical objects. This primarily includes variables to describe the state of the system and governing relationships between these variables. The number of independent variables within the system is referred to as the *degrees-of-freedom* or DOF. For example, the configuration of a single-degree-of-freedom

(SDOF) system can be determined using just one scalar variable; a multidegrees-of-freedom (MDOF) system needs to be defined using multiple scalar variables. In addition, a model gives mathematical equations to describe the governing relationships between these variables. For example, we can use constitutive relationships to correlate fold angles and crease moments or use kinematic constraining equations to coordinate folding angles between different creases. We are usually interested in how these variables evolve over "time" (or loading step) without violating the governing equations. However, a model alone cannot tell us how these variables evolve as it only formulates a mathematical problem to be solved. To further solve the evolution problem, solution methods are needed.

Solution method: We define solution methods as ways of solving mathematical problems. For sufficiently simple origami models, analytical solutions can be found for the folding motion. More complicated origami models, however, require the solution of partial differential equations or ordinary differential equations (ODEs) with no analytical solution. In such cases, numerical solution methods are used to analyze the problem.

Simulation: In general, simulation refers to imitating the behaviors of physical systems over time in virtual environments. More specifically, a simulation includes a model to represent a physical system and a solution method to solve how the system evolves over time (or loading step). A suitable origami model is developed based on the characteristics of the physical origami system and a solution method is chosen based on the characteristics of the mathematical problem embedded in the origami model.

**2.2 Origami Terminology.** Next, we introduce common origami terminologies, which will be used throughout the remainder of this paper.

Crease: The creases (or folds) of an origami pattern are the lines about which the folding occurs; see Figs. 2(a) and 2(b). Common origami models idealize creases as one-dimensional (1D) fold lines with zero width and the adjacent panels rotate about these creases. The terms "creases" and "folds" are often used interchangeably.

Compliant crease: Unlike creases that provide rotation about a 1D axis (like a door hinge), the folding motion of compliant creases relies on a distributed bending deformation over the width of a crease. The non-negligible width of these compliant creases requires additional considerations when building models for origami systems. Compliant membranes often serve as origami creases for actuation [19,21] or for panel thickness accommodation [67].

Vertex: The vertex is a "point" where multiple creases meet; see Fig. 2(b). In most origami models, the vertex is indeed a point

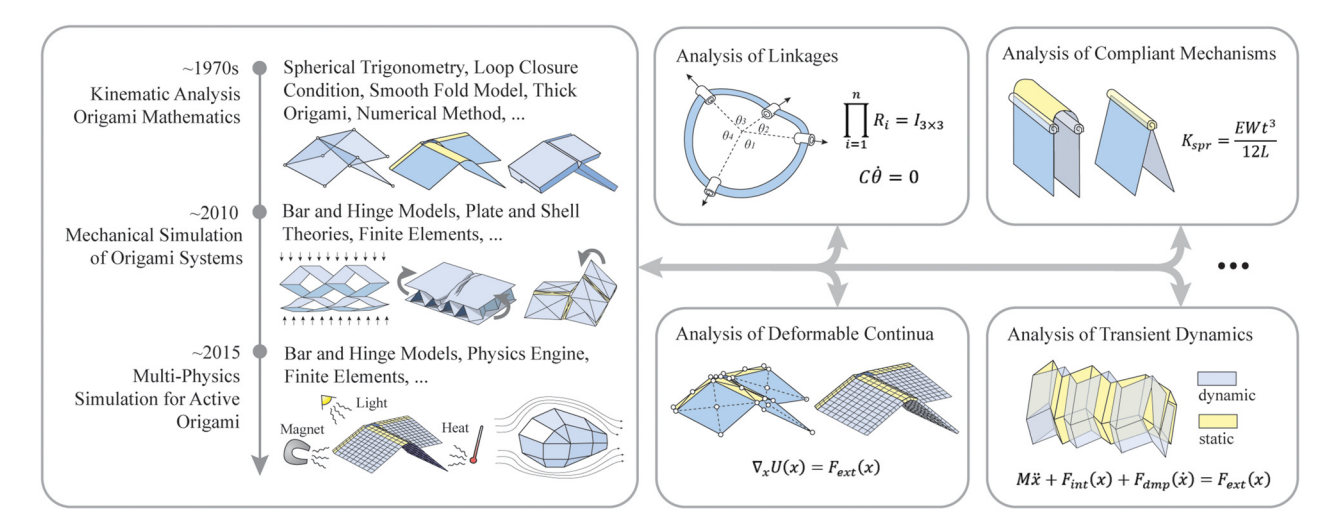


Fig. 1 The history of simulation of origami systems in a broad brush stroke (left) and related analysis methods and techniques from other engineering disciplines (right)

in 3D space. However, when modeling origami with thick panels or with compliant creases, the intersection of creases is no longer a defined point—nonetheless, a vertex can still be identified intuitively.

*Panel:* The panel is the facet of an origami pattern; see Fig. 2(b). For straight-crease origami, it is the polygon enclosed by origami creases and boundary lines.

Origami crease pattern: The crease pattern is the geometry formed by the vertices and creases of an origami in the flat configuration; see Fig. 2(a). In combination with the mountain/valley assignment of each of the folds, the crease pattern determines the folding motion of an origami pattern and has significant influence on the properties of an origami.

Mountain fold and valley fold: The mountain/valley fold convention denotes the direction of folding in origami. For example, the Miura-ori unit cell shown in Figs. 2(c) and 2(d) has three mountain folds, indicated with red solid lines, and one valley fold, indicated with blue dashed lines.

Sector angles: The sector angles are the in-plane angles around vertices used to describe origami patterns; see Fig. 2(c). In this work, we use  $\theta$  to represent sector angles.

Dihedral angles: The dihedral angle is the crease angle between two adjacent origami panels; see Fig. 2(d). It can be calculated using the normal vectors of the two adjacent panels. In this work, we use  $\phi$  to denote dihedral angles.

Fold angles: The fold angle is similar to the dihedral angle, but it measures how much a crease folds from its initial configuration. In general, the sum of the fold angle and the corresponding dihedral angle is 180 deg as indicated in Fig. 2(d). In this work, we use  $\rho$  to denote the fold angles.

*Thick origami:* Thick origami models integrate thickness into the model formulations for applications where the thickness of panels cannot be neglected.

*Rigid foldable origami:* An origami system is rigid foldable if the folding process can happen without panel deformation. That is, all deformations occur in the form of crease folding.

Developable origami: An origami pattern is developable if it forms a flat surface after all creases are unfolded (to flat). Equivalently, a developable origami pattern has all sector angles at each vertex adding to  $2\pi$ .

Flat foldable origami: An origami is flat foldable if it forms a flat surface after all creases are folded (to 180 deg). We will revisit developable origami and flat foldable origami in Sec. 3.

#### 3 Kinematics-Based Simulations

This section introduces kinematics-based simulations of origami systems. First, we briefly review how to perform kinematic

Fig. 2 Definitions of common origami terminologies

angle  $\phi$ 

simulations for a generic mechanism. Consider the analysis of the simple linkage shown in Fig. 3. The first step is to select the variables to describe its current configuration; here, we use the Cartesian coordinates (x, y) of the free moving end. Next, a kinematic constraining equation is established for the variables; here, the constraint is the fixed length l of the rigid member. After deriving this constraint, the kinematically admissible motion can be solved analytically or numerically. For an analytical solution, coordinate y can be directly calculated from coordinate x through rearranging the kinematic constraint. For a numerical solution, the constraining equations are first linearized with respect to time. Then, we find the kinematically admissible infinitesimal solution (the velocity solution of  $\dot{x}$  and  $\dot{y}$ ) which does not violate the linearized constraints. In this simple example, the velocity vector needs to be perpendicular to the rigid bar. Finally, an ODE solver can be used to solve how x and y vary over time. This simple example also illustrates how the selection of the variables can affect the solution process of the problem significantly; using polar coordinates here would have been more straightforward.

The remainder of this section addresses how to pick variables to represent an origami, how to form the constraining equations, and how to solve folding trajectories based on the constraining equations.

A key assumption in the kinematics-based simulations of origami is that the origami panels are assumed to be rigid throughout the folding process, meaning that the origami panels (or facets) do not change shape and remain planar. Usually, a kinematics-based origami model represents an origami structure using crease folding angles as variables. Based on the folding angles, kinematic constraining equations can be derived. Additional constraints can be added for enforcing developability and flat foldability of the origami pattern if necessary. These kinematic constraints will be relaxed when using mechanics-based simulations of origami systems where panel deformations are allowed. For sufficiently simple systems, the embedded mathematical problem can be solved directly and the evolution of the folding angles is found analytically. However, for more complicated systems, we often rely on numerical methods to solve for the folding trajectory.

In this section, we introduce different origami model formulations and solution methods used to analyze the kinematic folding motions of origami systems. The subsections are categorized based on the characteristics of the origami systems: (1) developable and flat-foldable origami; (2) thin and rigid origami; (3) compliant crease origami; and (4) thick origami. Subsection 3.1 introduces the constraining equations for developability and flat-foldability, and a simulation technique for solving this type of origami system. Subsections 3.2–3.5 introduce kinematic simulations for thin and rigid origami models (with rigid panels that have assumed zero thickness). More specifically, Subsecs. 3.2 and 3.3

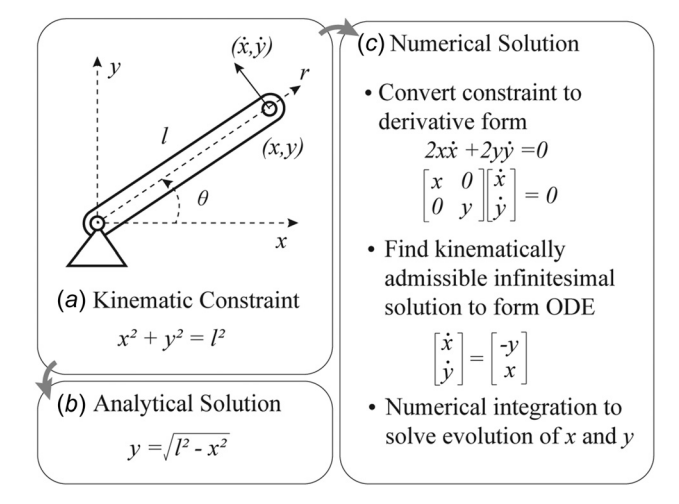


Fig. 3 An introduction to kinematics-based simulations

angle  $\theta$ 

Table 1 A summary of kinematics-based simulations for origami

	Table 1 A summary of kinemat	ics-based simulations for origami	
Simulation technique	Formulation	Notes	Reference
Flat-foldable origami Reflection based simulation	Reflection operations are used to capture the flat folding process of origami systems. The simulation checks if flat folding conditions are met and gives the overlapping conditions of panels.	The simulation technique does not predict intermediate folding steps and directly maps the developed flat configuration to another flat folded configuration.	References [57] and [68]. Left figure from Ref. [68]. Figure reproduced with permission from the authors.
Thin and rigid origami Spherical trigonometry	The folding angle of the origami is solved using spherical trigonometry directly (see Eqs. (4)–(7)).	This simulation is mostly used for analyzing SDOF systems and the origami kinematics are solved analytically.	References [10,32,51], and [69–80]. Left figure from Ref. [70]. Figure reproduced with permission from American Physical Society (2015).
Basic trigonometry	The nodal coordinates and folding angles of the origami are solved using basic trigonometry, where the nodal coordinates are included as model variables to simplify the derivation.	This simulation is usually applicable to specific patterns with periodically repeating unit cells.	References [5,41], and [81–83]. Left figure from Ref. [5]. Figure reproduced with permission from the authors.
Loop closure constraint	This simulation technique represents the loop closure constraint (Eq. (16)) using rotational matrix and solves the folding motion that complies with the constraining equation.	This constraint is mathematically equivalent to representing origami vertices using spherical trigonometry. Numerical solution methods can be used for MDOF systems.	References [53,55,56], and [84–96]. Left figure from Ref. [97]. Figure reproduced with permission from the authors.
Quaternions  (a) $E_1$ $O$	The loop closure constraint is expressed using quaternions instead of the rotation matrix.	Although using quaternions is less popular, prior work suggests that quaternions can be more efficient and can capture the panel contact [98].	References [98–101]. Left figure from Ref. [98]. Figure reproduced with permission from the Royal Society (2010).
Geometric-graph-theory $ \begin{bmatrix} 2 & & & & & & & & & & \\ A(K) & & & & & & & & & \\ & & & & & & & & & \\ & & & & $	The graph product is used to represent the origami geometry with periodic units, such as the (generalized) Miura-ori tessellation.	The simulation technique can capture the periodic folding motion in origami.	Ref. [102]. Left figure from Ref. [102]. Figure reproduced with permission from American Society of Mechanical Engineers ASME (2019).
Compliant crease origami Smooth fold model	The simulation technique is an extension of the loop closure constraint. In addition to the rotational constraint, a translational constraint is added to ensure compatibility at a vertex.	The formulation is similar to simulating openings in origami using a loop closure constraint. An extension of the model enables it to consider mechanical loading behaviors [103].	References [103–107]. Left figure from Ref. [103]. Figure reproduced with permission from American Society of Mechanical Engineers ASME (2017).
Thick origami Spatial linkages	The simulation technique captures the motion of degree-4, degree-5, and degree-6 thick origami vertices as spatial 4R, 5R, and 6R linkages.	This technique can capture thick origami made with a hinge-shift technique.	References [108] and [109]. Left figure from Ref. [108]. Figure reproduced with permission from American Association for the Advancement of Science AAAS (2015).
Rolling hinges	Kinematic constraining equations can be derived based on the geometry of the rolling surface and the motion can be solved analytically.	This technique is designed specifically for thick origami with rolling hinge connections.	References [110] and [111]. Left figure from Ref. [110]. Figure reproduced with permission from American Society of Mechanical Engineers ASME (2017).

Kinematic constraining equations can be derived based on the geometry of a 4-bar linkage and the motion can be solved analytically. This technique is designed specifically for offset linkage based thick origami systems. Reference [112]. Left figure from Ref. [112]. Figure reproduced with permission from American Society of Mechanical Engineers ASME (2020).

introduce simulations that are based on analytical solution methods while Subsecs. 3.4 and 3.5 focus on simulations that use numerical solution methods. After introducing the thin and rigid origami model, we will discuss how to extend this model to capture the behaviors of compliant crease origami (Subsec. 3.6) and thick origami systems (Subsec. 3.7). Table 1 gives a summary of kinematics-based simulations covered in this section.

3.1 Developable and Flat-Foldable Origami. The first simulation technique we will introduce is the reflection-based simulation for computing the folded configurations of developable and flat-foldable origami systems. Before introducing the formulation of this simulation technique, we further discuss developability and flat-foldability of origami patterns. These two concepts can be used to generate kinematic constraining equations for many origami models.

If an origami vertex is developable, it should form a flat surface when there is no folding at all creases. Equivalently, a developable origami vertex should have

$$\sum_{i=1}^{N} \theta_i = 2\pi \tag{1}$$

where  $\theta_i$  are the sector angles within the vertex. Figure 4(a) provides an intuitive explanation of this equation. If the sum of all sector angles is smaller than  $2\pi$ , a cone is obtained. If the sum of all sector angles is larger than  $2\pi$ , the additional angles will prevent the paper from reaching a flat configuration and a saddle-like configuration is obtained. A more mathematically rigorous definition for developability can be found in the textbook by Demaine and O'Rourke [113]. Developability is particularly valuable for the fabrication of origami structures: planar fabrication techniques

like lithography [20,21,25] or laser cutting [13,14] can be used to build the origami structure before folding it into a 3D shape.

Flat-foldability is another important characteristic of an origami vertex. An origami vertex is flat-foldable if it forms a flat surface after all creases are folded by  $\pm 180$  deg. The flat foldability is useful for densely packing engineering systems [28,35,114]. The Kawasaki–Justin theorem [54, 115] provides one necessary condition for a degree-n vertex to be flat-foldable

$$\theta_1 + \theta_3 + \dots + \theta_{n-1} = \theta_2 + \theta_4 + \dots + \theta_n = 180 \deg$$
 (2)

where n needs to be even. In addition to these angular relationships, the necessary mountain-valley assignment is given by the Maekawa theorem [116], which states that the number of mountain folds and valley folds should differ by  $\pm 2$ . Figure 4(b) gives a graphical explanation of these two theorems. The origami in Fig. 4(b) is a degree-4 vertex and has four sector angles,  $\theta_1$  to  $\theta_4$ . If the vertex is cut from a unit circle, then the arc lengths associated with these four sector angles are also  $\theta_1$  to  $\theta_4$ . For the vertex to be folded flat, the sum of arc lengths from odd sector angles should equal the sum of arc lengths from even sector angles, that is:  $\theta_1 - \theta_2 + \theta_3 - \theta_4 = 0$ . If this condition is not satisfied, the origami will be torn apart and develop a "gap" if forced to fold flat, as illustrated in Fig. 4(b). More rigorous mathematical proofs and derivations for flat-foldability can be found in Ref. [113]. Both developability and flat-foldability were discussed extensively in the early works on kinematic simulations of origami, such as in the work by Bern and Hayes [117], Hull [118], Kawasaki [54], and Justin [115].

Finding the flat folded configuration of a developable and flatfoldable origami can be done directly, as demonstrated in the work by Mitani [57]. In his work, a reflection-based simulation is used to generate the flat folded configuration of origami by using seven reflection based operations summarized in Ref. [57]. After

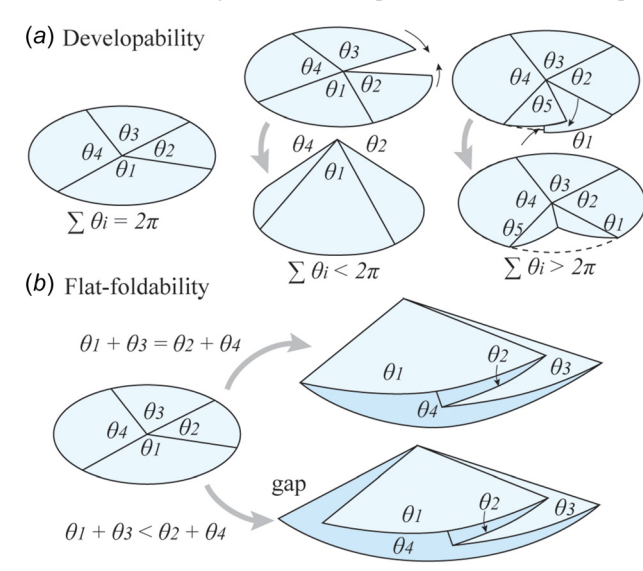


Fig. 4 Developability and flat-foldability of an origami with a single vertex

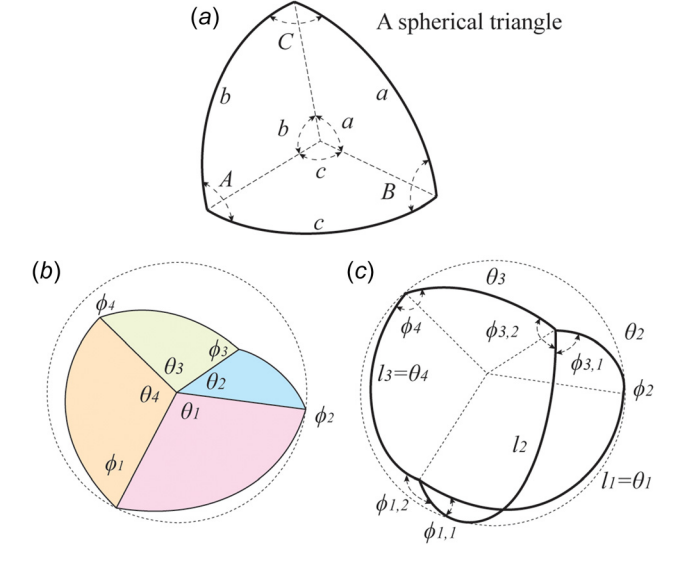


Fig. 5 Simulating origami folding using spherical trigonometry

generating the flat-folded configuration, one can determine the overlapping conditions of panels using a brute-force searching approach. This simulation technique is implemented in a JAVA software package called ORIPA and can be found at Ref. [68]. The reflection-based simulation was later used to study the folding of curved crease origami by Mitani and his coworkers [119]. Although the simulation was one of the early achievements in the field of computational origami, it cannot reproduce the intermediate folding process.

3.2 Spherical Trigonometry and Analytical Methods. Not all origami systems are developable or flat-foldable, and these constraints can therefore be relaxed. For thin and rigid origami system, the only assumption is that the panels of the origami are rigid with zero thickness. In this section, we introduce the use of spherical trigonometry to capture this thin and rigid origami system.

Spherical trigonometry provides one direct way of simulating the folding motions of a thin and rigid origami system [70,74]. We represent the relationship between crease dihedral angles at a vertex using spherical trigonometry and solve how these dihedral angles evolve analytically. Figure 5(a) shows a spherical triangle, which is the intersection of a three-face box corner and a unit sphere. Angles a, b, and c are the angles of the three-face box corner measured at the center of the sphere, while the angles A, B, and C are the angles measured on the curved surface of the sphere (using the tangent line of the great circle arc). For a unit sphere the arc lengths corresponding to the center angles a, b, and c are also a, b, and c. These angles (or arc lengths) can be related using the cosine rule

$$\cos(a) = \cos(b)\cos(c) + \sin(b)\sin(c)\cos(A),$$
  

$$\cos(b) = \cos(a)\cos(c) + \sin(a)\sin(c)\cos(B),$$
  

$$\cos(c) = \cos(a)\cos(b) + \sin(a)\sin(b)\cos(C).$$
(3)

Using these relationships, we can directly solve for the dihedral angles of creases. For the degree-4 vertex shown in Fig. 5(b), applying the spherical trigonometry equations with added arc  $l_2$  (see Fig. 5(c)) allows us to relate the dihedral angles of these four creases as

$$\phi_{1} = \phi_{1,1} + \phi_{1,2} = \cos^{-1} \left( \cos(\theta_{2}) - \frac{\cos(l_{2})\cos(l_{3})}{\sin(l_{2})\sin(l_{3})} \right) + \cos^{-1} \left( \cos(\theta_{3}) - \frac{\cos(l_{1})\cos(l_{2})}{\sin(l_{1})\sin(l_{2})} \right)$$
(4)

$$\phi_2 = \cos^{-1}\left(\frac{\cos(l_2) - \cos(\theta_1)\cos(\theta_2)}{\sin(\theta_1)\sin(\theta_2)}\right)$$
 (5)

$$\phi_{3} = 2\pi - \phi_{3,1} - \phi_{3,2}$$

$$= 2\pi - \cos^{-1}\left(\frac{\cos(l_{1}) - \cos(l_{2})\cos(\theta_{2})}{\sin(l_{2})\sin(\theta_{2})}\right)$$

$$-\cos^{-1}\left(\frac{\cos(l_{3}) - \cos(l_{2})\cos(\theta_{3})}{\sin(l_{2})\sin(\theta_{3})}\right)$$
(6)

$$\phi_4 = \cos^{-1}\left(\frac{\cos(l_2) - \cos(\theta_3)\cos(\theta_4)}{\sin(\theta_3)\sin(\theta_4)}\right) \tag{7}$$

These equations are obtained by applying the cosine rules to the two spherical triangles marked with arc  $\{\theta_1,\theta_2,l_2\}$  and  $\{\theta_3,\theta_4,l_2\}$  of the degree-4 vertex. Generic equations for an arbitrary degree-n vertex can be found in Refs. [70,75]. For simplicity, we will focus on the degree-4 vertex. Assuming that all sector angles are given, it can be seen from the above four equations that the degree-4 vertex has a single degree-of-freedom.

Although this simulation is derived for more generic thin and rigid origami systems, it can still be applied to developable and flat-foldable origami systems. Substituting the developability and flat-foldability constraints for a degree-4 vertex,  $\theta_1 + \theta_3 = \pi$  and  $\theta_2 + \theta_4 = \pi$ , into Eqs. (4)–(7) will yield

$$\phi_1 = -\phi_3$$
$$\phi_2 = \phi_4$$

which shows that that the dihedral angles at the opposite sides of such a degree-4 vertex are equal [32,51,69,72]. By convention, folds 1 and 3 are referred to as minor folds and folds 2 and 4 as major folds. The minor folds have opposite mountain-valley assignments while the major folds have the same assignments.

For this developable and flat-foldable degree-4 vertex, we can further express the relation between dihedral angles  $\phi_1$  and  $\phi_2$  using the *fold angle multiplier*  $\mu_{1,2}$  as

$$\mu_{1,2} = \frac{\tan\left(\frac{1}{2}\phi_1\right)}{\tan\left(\frac{1}{2}\phi_2\right)} = \frac{\sin\left(\frac{1}{2}(\theta_1 + \theta_2)\right)}{\sin\left(\frac{1}{2}(\theta_1 - \theta_2)\right)}$$
(8)

The general form of dihedral angle multiplier  $\mu_{i,j}$  and the calculation of the remaining three folding angle multipliers for the degree-4 vertex are

$$\mu_{i,j} = \frac{\tan\left(\frac{1}{2}\phi_j\right)}{\tan\left(\frac{1}{2}\phi_i\right)} \tag{9}$$

$$\mu_{3,4} = -\mu_{1,2}; \ \mu_{2,3} = -\frac{1}{\mu_{1,2}}; \ \mu_{4,1} = \frac{1}{\mu_{1,2}}$$
(10)

This fold angle multiplier is thoroughly discussed in Ref. [72]. Different derivations (such as using Gaussian Sphere) of this angular relationship on minor and major folds can be found in the textbook by Hull [74] (Activities 29 and 30) and in the appendix by Lang et al. [32].

The fold angle multiplier provides a useful technique to extend the study of a single vertex to the study of an entire origami pattern [72]. To further ensure that the vertices around a polygonal panel are rigid foldable, we need to ensure that

$$\prod_{i=1}^{n} \mu_i = 1 \tag{11}$$

where  $\mu_i$  are the fold angle multiplier of the angles within a polygonal panel. Figure 6 shows an example based on the Miura-ori tessellation. Using Eqs. (8) and (10), the fold angle multipliers of the Miura-ori unit cell are calculated. Next, we place these values at the corresponding locations on the pattern. To ensure that the four vertices around a quad panel can fold, we need to have  $\mu_1\mu_2\mu_3\mu_4 = 1$ . In this example, the Miura-ori pattern indeed satisfies the requirement and thus it is rigid foldable.

This fold angle multiplier is particularly useful for designing and studying the kinematics of quad-based developable and flat-foldable origami, which are origami patterns with degree-4 vertices and quadrilateral panels [69,71]. Based on this fold angle multiplier, Evans et al. summarize various rigid-foldable quad-based origami patterns (such as the Miura pattern, Huffman grid pattern, chicken wire pattern) and introduce multiple ways to adjust these existing patterns for developing new patterns in Ref. [71]. Similar but equivalent techniques for quad-based origami systems were also developed by Tachi [73], Lang et al. [69], and Feng et al. [87].

**3.3 Trigonometry and Analytical Methods.** The simulation techniques introduced in Subsec. 3.2 only use dihedral angles to

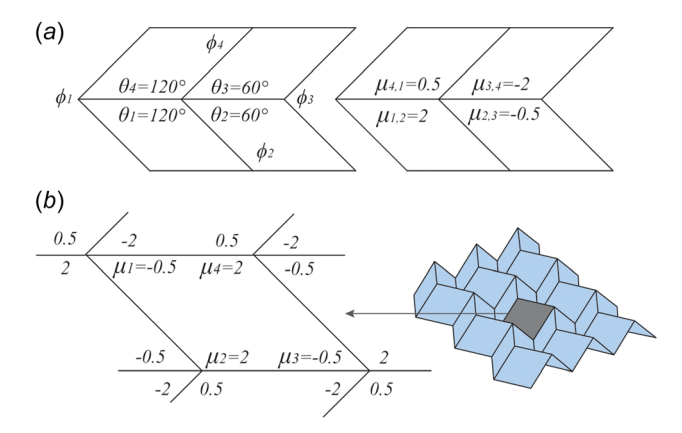


Fig. 6 Applying the fold angle multiplier to analyze the folding motion of an Miura origami pattern

describe the folded geometry of an origami structure. It is common to further include the nodal coordinates as model variables for representing the configurations of origami structures when working on simple patterns with repeating unit cells [5,10,62]. For example, the folding motions of Miura-ori patterns can be calculated using standard trigonometry and the nodal coordinates of the Miura unit are found using the following equations [5]:

$$H = a \cdot \sin(\psi)\sin(\theta) \tag{12}$$

$$S = b \cdot \frac{\cos(\psi)\tan(\theta)}{\sqrt{1 + \cos^2(\psi)\tan^2(\theta)}}$$
 (13)

$$L = a \cdot \sqrt{1 - \sin^2(\psi) \sin^2(\theta)}$$
 (14)

$$V = b \cdot \frac{1}{\sqrt{1 + \cos^2(\psi) \tan^2(\theta)}} \tag{15}$$

where the variables are depicted in Fig. 7. Solving the nodal coordinates of an origami structure directly is useful in some situations. For example, the above equations relate the length 2L and width 2S of the unit cell, so the Poisson's ratio of Miura-ori metamaterials can be found directly [5,10,62]. However, direct calculation of the nodal coordinates is usually only applicable to simple patterns with repeating unit cells such as the Miura-ori and its variations [81,82]. In special situations, this approach can also be applied to study the folding motions of specific patterns such as the shopping bag packing problem in Refs. [41] and [83].

The simulation techniques introduced in Subsecs. 3.2 and 3.3 are primarily suitable for analyzing the folding motion of SDOF origami patterns because analytical solution methods are used. Certain origami patterns with higher degree vertices (and therefore MDOF kinematics) can also be solved analytically by introducing additional symmetry constraints. Symmetry constraints enforce the same folding angles in specific sets of creases, which reduce the kinematics to SDOF. For instance, the waterbomb pattern (which contains degree-6 or degree-8 vertices) has been studied by adding symmetry conditions [120], which have revealed

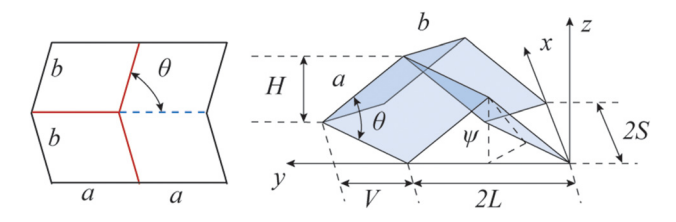


Fig. 7 Geometry of Miura-ori using standard trigonometry

multistability [79] and the ability to program 3D surfaces [121]. Wang et al. have given a summary of various patterns with degree-6 vertices [122].

3.4 Loop Closure Constraint and Numerical Methods. In order to create a simulation technique for generic origami systems with MDOF kinematics, a more scalable and compact formulation of the kinematic constraints is required. Over the years, origami researchers have realized that the study of origami systems shares great similarities with the study of linkages [88–90,113]. More specifically, a thin and rigid origami vertex can be represented by an equivalent spherical linkage model (Fig. 8). This similarity provides an approach to construct the loop closure constraint, which can be solved using numerical methods. The mathematical equation of loop closure constraint is first developed by Kawasaki [53] and Belcastro and Hull [55] without highlighting the connection with spherical linkages.

Figure 8 demonstrates how the loop closure constraint for an origami matches that of a spherical linkage. In this formulation, the loop closure constraint can be represented using rotation matrices as

$$\mathbf{F}(\rho_1, ..., \rho_n) = \mathbf{R}_{3,n} \mathbf{R}_{1,n} ... \mathbf{R}_{3,1} \mathbf{R}_{1,1} = \mathbf{I}_{3 \times 3}$$
 (16)

where  $\mathbf{R_{1,i}}$  and  $\mathbf{R_{3,i}}$  are defined as

$$\mathbf{R}_{\mathbf{1},\mathbf{i}} = \begin{bmatrix} 1 & 0 & 0 \\ 0 & \cos \rho_i & -\sin \rho_i \\ 0 & \sin \rho_i & \cos \rho_i \end{bmatrix}$$
(17)

$$\mathbf{R_{3,i}} = \begin{bmatrix} \cos\theta_i & -\sin\theta_i & 0\\ \sin\theta_i & \cos\theta_i & 0\\ 0 & 0 & 1 \end{bmatrix}$$
 (18)

The two matrices describe the rotation around local coordinate axis 1 and axis 3 of a folding crease as shown in Fig. 8 (counter-clockwise). In addition to using the plain rotational matrix, it is also popular to represent the same constraint using the Denavit–Hartenberg transformation matrix (with additional displacement variables) [88,90,108] or other mathematically equivalent representations such as those demonstrated in Feng et al. [87]. For simplicity, we will use the simple rotational matrix based representation here.

To understand this equation, imagine that we walk around the vertex. Every time we cross the panel with sector angle  $\theta_i$  we rotate about axis 3 using  $\mathbf{R}_{3,i}$ , and every time we cross a crease  $\phi_i$ , we rotate by fold angle  $\rho_i$  about axis 1 using  $\mathbf{R}_{1,i}$ . Thus, the relationship between the adjacent crease direction vectors  $\mathbf{e}_i$  and  $\mathbf{e}_{i+1}$  can be expressed as  $\mathbf{e}_{i+1} = \mathbf{R}_{3,i}\mathbf{R}_{1,i}\mathbf{e}_i$ . In this fashion, if we combine all the rotations around a given vertex, we should have

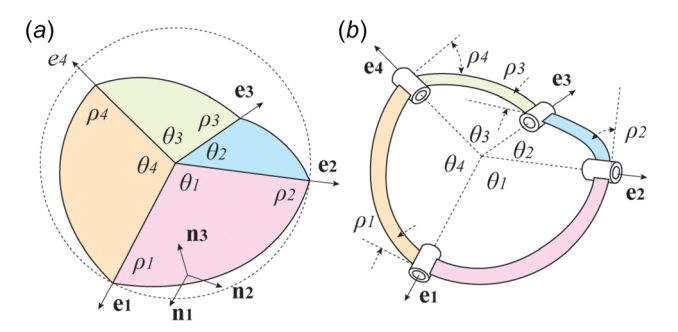


Fig. 8 Simulating "thin and rigid" origami vertex as a spherical linkage. (a) An origami system. The vectors  $n_1, n_2, n_3$  denote a local coordinate system for the first panel (corresponding to  $\theta_1$ ), where  $n_1 \parallel e_1$  and  $n_3$  is perpendicular to the panel. (b) The corresponding sphericallinkage model.

 $R_{3,n}R_{1,n}...R_{3,1}R_{1,1}e_1=e_1$ , which is equivalent to saying that  $R_{3,n}R_{1,n}...R_{3,1}R_{1,1}$  equals the identity matrix. Or in terms of walking, we return to the starting position.

There are a few properties worth mentioning regarding this loop closure constraint. First, this constraining equation is applicable to an arbitrary degree-n vertex (including nondevelopable vertices). Second, the loop closure constraint is mathematically equivalent to using spherical trigonometry, as pointed out in Refs. [56] and [69]. Third, Eq. (16) gives three constraining equations for a single vertex so a generic degree-n vertex will have n-3 degrees-of-freedom. Finally, to extend this loop closure constraint from a vertex to an entire pattern, we need to ensure that all internal vertices of the pattern satisfy the constraint.

Now that we have the loop closure constraint, we can follow the process identified in Fig. 3(c) to solve for the folding motion numerically. First, taking the derivative of the loop closure constraint with respect to time (Eq. (16)) will give a linearized constraining equation. This equation shows how the loop closure constraint acts on the folding velocity of each fold. Next, we identify the nontrivial solution of the folding velocity that satisfies the linearized constraint. Finally, we numerically integrate this folding velocity solution to solve for the folding motion.

With this general process in mind, the first task is to calculate the derivative of this loop closure constraint to obtain the following governing equation:

$$\mathbf{C}\dot{\boldsymbol{\rho}} = \begin{bmatrix} \begin{bmatrix} \mathbf{C}_1 \\ \vdots \\ \begin{bmatrix} \mathbf{C}_M \end{bmatrix} \end{bmatrix} \begin{bmatrix} \dot{\boldsymbol{\rho}}_1 \\ \vdots \\ \dot{\boldsymbol{\rho}}_N \end{bmatrix} = 0 \tag{19}$$

where the matrix  $\mathbf{C}$  is the Jacobian of the loop closure constraint, M is the number of vertices, N is the number of creases, the matrix  $[\mathbf{C_k}]$  is the derivative matrix for the kth vertex, and  $\dot{\rho_i}$  is the folding velocity of the ith crease. Details of the calculation can be found in Ref. [56].

The next task is to find the velocity vector  $\dot{\boldsymbol{\rho}}$  that satisfies this linearized constraining equation. Equation (19) shows that the solution must lie in the null space of the Jacobian C to satisfy the loop closure constraint. Following the work by Tachi, this nontrivial solution of  $\dot{\boldsymbol{\rho}}$  is calculated using a trial velocity vector  $\dot{\boldsymbol{\rho}}_0$  and the pseudo-inverse of matrix C as

$$\dot{\boldsymbol{\rho}} = [\mathbf{I}_{\mathbf{N}} - \mathbf{C}^{+}\mathbf{C}]\dot{\boldsymbol{\rho}}_{0} \tag{20}$$

where  $\dot{\rho}$  is the projection of the trial vector  $\dot{\rho}_0$  onto the null space of the constraint matrix C. By selecting different trial vectors  $\dot{\rho}_0$ , one can also track different folding trajectories and study the bifurcation of different folding paths.

Finally, to find the evolution of the folding angles over time, we numerically integrate the folding velocity  $\dot{\rho}$ . There are numerous solution methods available to handle this ODE. Tachi [56] used Euler's method to simulate the motion of rigid origami, and many coding packages provide built-in ODE solvers such as the ode45 function in MATLAB. In addition to these methods, Hu et al. introduce a Lagrange multiplier-based method to calculate the

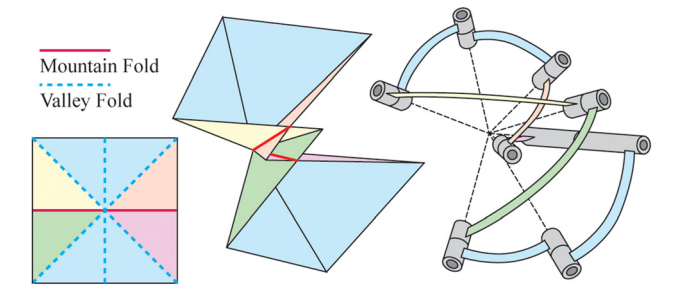


Fig. 9 Loop closure based simulation techniques cannot capture situations where panels intersect

folding trajectory [85]. Xi and Lien give a solution method that uses the pattern symmetry to speed up the algorithm when searching for the folding trajectory [86].

This loop closure-based simulation has enabled numerous works on the design of origami systems. In subsequent work by Tachi and Demaine [91–93], they developed an approach to tuck fold an origami pattern to fit arbitrary surfaces based on this simulation. Feng et al. studied helical Miura origami [95] using an equivalent loop closure formulation [87]. Their modified formulation was also used in Ref. [123] to study the folding motion of an origami-inspired shape memory alloy medical stent. Silverberg et al. studied the mechanical behaviors of origami by adding rotational springs to the kinematic relationships derived based on the loop closure constraints [96].

It should be noted that the numerical integration of the loop closure conditions described here cannot be applied directly to quadbased origami patterns with SDOF kinematics. This simulation technique relies on the existence of a null space in the Jacobian matrix C, to follow the folding motion. Due to the numerical errors accumulated in the simulation, the constraining equation may no longer be singular for quad-based origami systems. To avoid this, Tachi suggests triangulating the quad panels by introducing additional crease lines [56,84]. In this way, the SDOF quad-based origami is modeled as a MDOF system.

Finally, we wish to point out one fundamental limitation of the trigonometry-based simulations and the loop closure-based simulations. Both techniques cannot guarantee that the origami pattern is folded to a valid configuration. This is because the mathematical theories behind both simulations do not consider the intersection of panels at a vertex and thus only provide necessary but nonsufficient conditions for having a valid folding process [55,113] (see Fig. 9). More difficulties emerge when considering intersections between different parts of the origami that do not share a single vertex. The search of a sufficient and necessary condition for folding a thin and rigid origami remains an open question [113].

3.5 Other Simulations for Thin and Rigid Origami. In addition to the use of spherical trigonometry and loop closure constraints, other simulations have also been developed to study the kinematics of rigid and thin origami structures. Although these simulations utilize different mathematical representations for the thin and rigid origami model, their formulations remain mathematically equivalent.

Wu and You [98] first used quaternions to describe the kinematics of thin and rigid origami, replacing the rotation matrices when expressing the loop closure constraint. Using quaternions offers a number of advantages when compared to rotation matrices. For example, quaternions give more compact representations of rigid body rotations, are numerically more stable and allow users to potentially determine panel intersection to rule out invalid origami configurations [98]. The quaternion-based simulation was used to study Miura-ori inspired structures and to demonstrate the nonrigid-foldability of Kresling patterns in the works by Cai et al. [100,101]. Despite their benefits, quaternions have not been popular among the origami community, likely because engineers and scientists are less familiar with this mathematical tool.

More recently, a paper by Chen et al. [102] demonstrated a new approach for representing the geometry of origami using an integrated geometric-graph-theoretic approach. In this approach, the graph product is used to generate the origami pattern with periodic geometries. The paper applies this approach to study the folding motion of the Miura-ori and Kresling patterns. However, the current formulations have difficulties representing origami with non-periodic characteristics (i.e., free-form origami patterns [91]). The use of this graph product-based approach provides an efficient technique for studying the uniform folding behavior (as well as the corresponding loading behavior under uniform load), but future studies are needed to extend the formulation to capture non-periodic patterns.

3.6 Openings and Compliant Creases. If the origami has internal openings or contains compliant creases, new constraints, in addition to the loop closure constraint (Eq. (16)) are needed to ensure valid folded configurations. In previous works on the simulations of origami with internal openings and compliant creases, the two topics are discussed separately. However, a closer look at the formulations of these two techniques will reveal that they share great similarities.

Figure 10(a) shows an origami loop with an opening. A loop pattern like this can be modeled as a spatial linkage [88]. As pointed out by Tachi [84], an additional constraint is required in addition to the loop closure condition in Eq. (16). This extra constraint takes the form of

$$\sum_{k=1}^{n} \left( \prod_{i=1}^{k} \left( \mathbf{R}_{1,i}(\rho_i) \mathbf{R}_{3,i}(\theta_i) \right) \mathbf{d}_k \right) = \mathbf{0}_{3 \times 1}$$
 (21)

where  $\mathbf{d}_k$  is the edge vector following the internal loop boundary. The edge vector  $\mathbf{d}_k$  is expressed in the local facet coordinate system and can be zero, as illustrated in Fig. 10(a). The rotation  $\Pi_{i=1}^k \left(\mathbf{R_{1,i}}(\rho_t)\mathbf{R_{3,i}}(\theta_i)\right)$  is applied to  $\mathbf{d}_k$  to express it in the global coordinate system. In effect, this additional Eq. (21) ensures that we return to the location where we started after looping around the opening and the original loop closure Eq. (16) ensures that we recover a direction that is parallel to the starting orientation. A single vertex discussed in Subsecs. 3.1–3.5 is a special case of the loop pattern with an opening where all edge vectors  $\mathbf{d}_k$  are zero and Eq. (21) is therefore automatically satisfied. This modeling technique for origami patterns with openings enables the design of "geometrically misaligned" patterns, which are origami patterns with missing panels, proposed by Saito et al. [124].

Figure 10(b) gives an illustration of a single vertex with compliant creases. Similarly, in addition to the rotational constraint expressed in Eq. (16) another translational constraint is needed. This additional constraint was developed by Hernandez et al. [103] and is referred to as the "smooth fold model." This constraint has the form

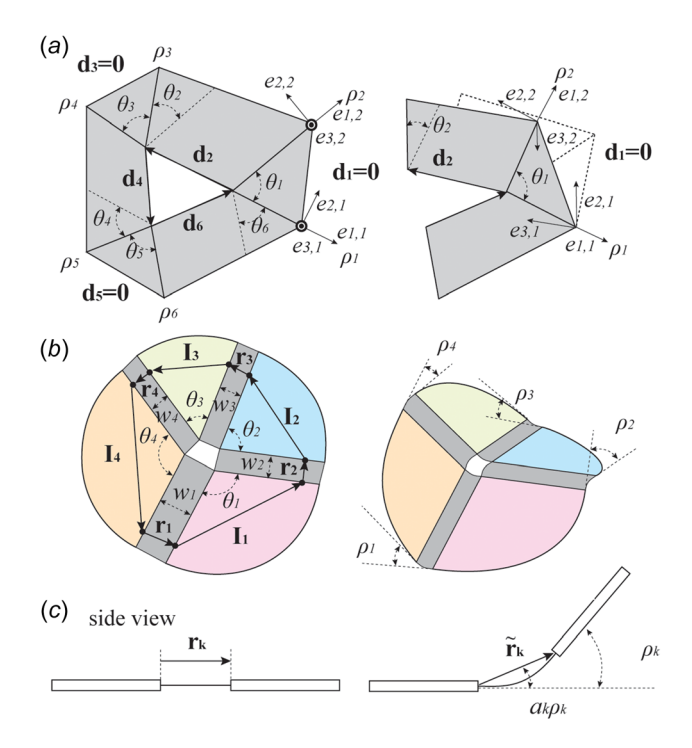


Fig. 10 Origami with openings (a), and those with compliant creases (b) and (c) can be modeled similar to spherical linkages, but with additional constraints

$$\sum_{k=1}^{n} \left( \prod_{i=1}^{k-1} \left( \mathbf{R}_{\mathbf{1},\mathbf{i}}(\rho_i) \mathbf{R}_{\mathbf{3},\mathbf{i}}(\theta_i) \right) \mathbf{R}_{\mathbf{1},\mathbf{k}}(a_k \rho_k) \widetilde{\mathbf{r}_k} \right) + \prod_{i=1}^{k-1} \left( \mathbf{R}_{\mathbf{1},\mathbf{i}}(\rho_i) \mathbf{R}_{\mathbf{3},\mathbf{i}}(\theta_i) \right) \mathbf{R}_{\mathbf{1},\mathbf{k}}(\rho_k) \mathbf{I}_{\mathbf{k}} \right) = \mathbf{0}_{3\times 1}$$
(22)

where  $\widetilde{r_k}$  is a reference vector in the creases and  $I_k$  is a reference vector in the panels (both expressed in local coordinates). The rotation matrices in front of the two vectors convert them back to the same global coordinates. Setting the sum of all vectors to a zero vector ensures that the loop around the compliant crease vertex is not broken.

Detailed calculations of the reference vectors  $\tilde{\mathbf{r}_k}$  can be found in the original work [103]. In a nutshell, a polynomial deformation shape function is used to describe the compliant crease geometry, and this shape function is used to calculate  $\tilde{\mathbf{r}_k}$  and  $a_k$  based on the crease rotation and the width of crease. Hernandez et al. have enabled this model to further capture the strain energy stored within compliant creases for capturing mechanical loading [104]. This simulation technique was used for designing 3D surfaces for different engineering applications [105–107].

The above discussion shows that simulating the openings within origami patterns and the compliant capturing requires adding an additional vector-based constraining equation. The additional constraint is needed because the "vertex" has higher degrees-of-freedom for both cases. Therefore, even if the rotational constraint is satisfied, the linkage can still be broken due to translational motions. If we think of these origami vertices as spatial linkages, these additional translational constraints are related to the translation terms in the Denavit–Hartenberg transformation matrix, which is omitted when using the simple rotational matrix representation of the loop closure constraint. Moreover, if we can close the vertex by removing the opening [84] or by removing the width of the creases [103], both models can be reduced to the loop closure constraint shown in Eq. (16) and the constraints given in Eqs. (21) and (22) will be satisfied automatically.

3.7 Thick Origami. In this subsection, we discuss techniques for simulating thick origami structures. In general, different thickness accommodation techniques need to be captured using different approaches. Therefore, this subsection is organized based on the classification of different techniques for accommodating panel thickness (see Fig. 11) as provided in the review article by Lang [125].

We begin with two simple thickness accommodation techniques: the tapered panel technique [126] and the offset panel technique [127,128]. The thick origami systems generated using these two techniques have the same kinematic folding motions as their corresponding thin origami systems. Thus, any simulation technique for thin and rigid origami systems (those introduced in Subsecs. 3.2–3.5) can be used to solve the folding motion of these two types of thick origami. One limitation to consider is that, the range of the folding angle can no longer reach 180 deg when using the tapered panel technique [126].

Next, the double crease technique is also used for creating thick origami structures [129,130]. Here, the single crease is separated into two creases to accommodate the thick panels. Although the technique itself does not preserve the kinematics (because one crease is separated into two), the generated new crease pattern with double creases can still be analyzed with the loop closure constraint as demonstrated in the paper by Ku and Demaine [129]. In this case, the incorporation of double creases will generate openings within the origami pattern and thus the additional constraints for the openings (introduced in Subsec. 3.6) are required to capture the behavior accurately.

The rolling contact technique and the offset linkage technique are two approaches to build thick origami that have unique kinematics. Because of the special designs of these two thickness accommodation techniques, both rotational and translational motion occurs between adjacent panels during the folding process.

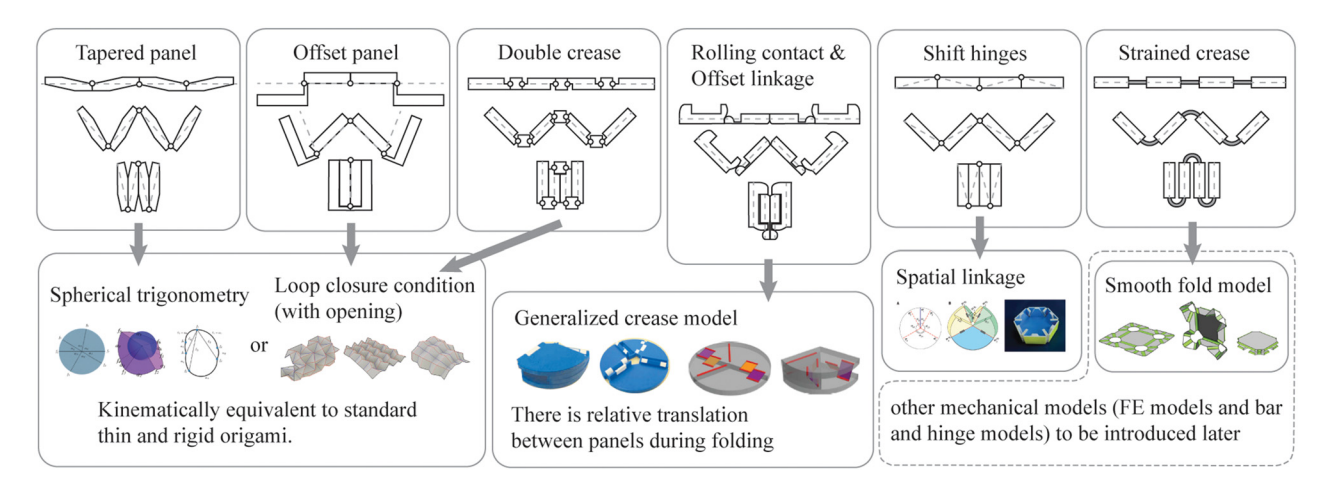


Fig. 11 Design and modeling techniques for thick origami systems. The copyright information for the bottom row figures is as follows. Spherical trigonometry figure [70] reproduced with permission from American Physical Society APS (2015); loop closure condition figure [97] reproduced with permission from the authors; generalized crease model [110,112] reproduced with permission from American Society of Mechanical Engineers ASME (2017) and (2020); spatial linkage figure [108] reproduced with permission from American Association for the Advancement of Science AAAS (2015); smooth fold model [103] reproduced with permission from American Society of Mechanical Engineers ASME (2017).

Thus, capturing the folding kinematics requires using a generalized crease model that can further consider the additional translational motion between adjacent panels. When using the rolling contact technique, the two adjacent panels each have a curved edge and can roll against each other [110]. The paper by Cai [111] and the work by Lang et al. [110] provide kinematic models and the analytical solutions for origami systems built with rolling contact. When using the offset linkage technique, the two adjacent panels are connected using a four bar linkage [112]. The work by Lang et al. [112] provides an approach to capture the kinematics of an offset linkage.

When using hinge-shift techniques, the hinges of the origami structures are placed on the opposite side of the panels to accommodate the thickness [108,131]. When the origami pattern is sufficiently simple (such as the Miura-ori pattern with symmetric bird foot vertices), the technique can be applied directly to accommodate the thickness as demonstrated in Ref. [131]. In this case, using the thin and rigid origami model to analyze the folding

kinematics is sufficient. However, when more complex vertices are encountered, one needs to rely on more sophisticated models to capture the folding kinematics. In the pioneering paper by Chen et al., they showed that the folding motions of thick origami vertices built with hinge-shift techniques can be captured using wellestablished spatial linkage models [108]. In their work, the degree-4, degree-5, and degree-6 thick origami vertices are modeled as spatial 4R, 5R, and 6R linkages. In this case, using the Denavit–Hartenberg transformation matrix with the additional displacement variable is helpful for representing the offset in thick panels [108]. With this modeling technique, the folding kinematics of these thick origami vertices can be solved using analytical methods. A summary of existing mechanical linkages can be found in Ref. [109].

Finally, we introduce the strained crease technique. Instead of using a hinge to connect adjacent panels, this technique connects two thick panels with a bendable soft plate to serve as a crease [67,132]. A design like this is commonly seen in active origami

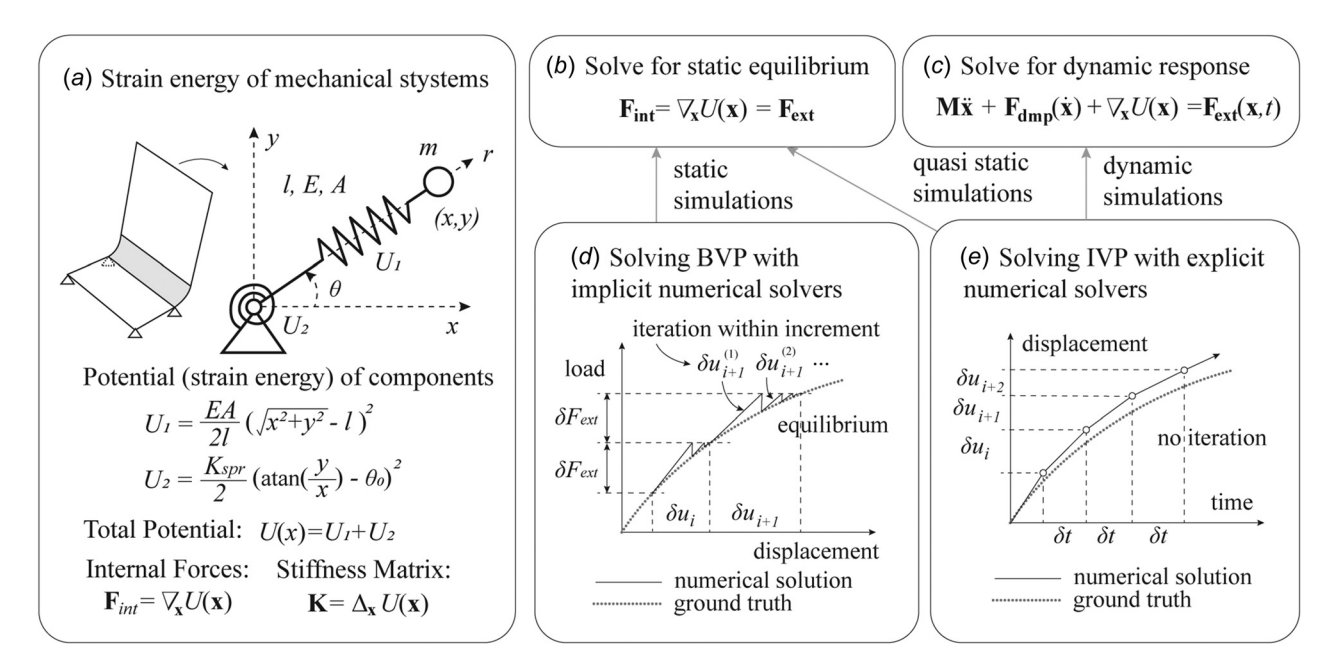


Fig. 12 An introduction to mechanics-based simulations of physical systems

Table 2 A summary of mechanics-based simulations and models for origami

Models	Formulation	Note	Reference
Rigid panel based models			
Rigid bar based models	This technique uses rigid bars to form triangulated origami panels	The technique represents a transition from kinematic to mechanic	References [61], [141] and [142]. Figure on the left is from Ref.
577	for solving the folding kinematics.	models and is a precursor to the bar	[141]. Figure reproduced with per
		and hinge model.	mission from Elsevier (2018).
Rigid frame based models	This model represents rigid origami	Rigid frame elements are used to	References [143] and [144]. Left
Com 3	panels using rigid frame elements and captures creases as rotational	preserve the folding kinematics. Correlating frame deformations to	figure from Ref. [143]. Figure reproduced with permission from
or respective of the state of t	hinges.	panel deformations is challenging within the current model.	Elsevier (2021).
Bar and hinge models			
Standard bar and hinge model	This model places bar elements	Bar and hinge model based simula-	References [43], [62], [63], and
K 5	between vertices to capture panel stretching and shearing and uses rotational spring elements to cap- ture crease folding and panel bending.	tions are computationally efficient and can capture the global mechani- cal behavior of origami.	[145–157]. Left figure from Ref. [63]. Figure reproduced with permission from the Royal Society (2017).
Compliant crease bar and hinge model	This model represents the geometry	This model can capture the bistabil-	References [64], [135], [136], and
compliant crease out and image model	of compliant creases by adding additional bar elements and rotational spring elements in the crease region.	ity and multistability possible from having compliant creases.	[158]. Left figure from Ref. [136]. Figure reproduced with permission form the authors.
Particle bar and hinge model	This model lumps the mass of the	Particle bar and hinge model based	References [159–165]. Left figure
Perfect Gallery	origami onto the nodes for captur- ing the dynamic behaviors of	simulations can analyze the transient dynamics of origami rapidly.	from Ref. [164]. Figure reproduce with permission from Elsevier
The state of the s	origami.	one of managers	(2021).
Plate theory based models			
Plates models for creases	This technique represents the origami compliant crease as a plate.	The technique can be used to calculate spring stiffness for bar and	References [166] and [167]. Left figure from Ref. [167]. Figure
	Analytical solutions of the deformation and stiffness are found.	hinge models as shown in [166]	reproduced with permission from Elsevier (2021).
Plates models for panels	This technique captures the small-	This formulation can be seen as a	References [145], [168], and [169]
	strain bending behavior of origami panels using plate theory.	coarse meshed FE model with limited capability for nonlinearity, but with improved efficiency.	Left figure from Ref. [168]. Figure reproduced with permission from Springer Nature (2021).
Finite element models	Th: - f	Th: f	D-f
Shell element panels and hinges	This formulation models origami panels using shell elements and ori-	This formulation is suitable for studying origami systems with	References [28], [145], [170], and [171]. Left figure from Ref. [170].
Shell Fold joint	gami creases as rotational springs or rotational hinges.	softer creases. The fold lines can deform or buckle under applied loading.	Figure reproduced with permission from the Royal Society (2016).
Shell element panels and rigid creases	This formulation models origami	This formulation is widely used for	References [139] and [172–188].
	systems as shell elements connected with rigid creases (that do not fold).	capturing origami unit cells and sheets [172–175], metamaterials [139,176–178], sandwich cores [179–182], and crash boxes [183–186] when the creases are rigidly connected.	Left figure from Ref. [188]. Figure reproduced with permission from Elsevier (2018).
Shell elements for both panels	This formulation represents both	This formulation is useful for cap-	References [104], [135], [136], an
and creases	creases and panels using shell ele- ments so that the compliant creases can be captured.	turing active origami with compli- ant creases as actuators.	[189]. Left figure from Ref. [189]. Figure reproduced with permission from American Society of Mechanical Engineers ASME (2016).

This formulation captures origami using solid type elements so that the model can capture the nonnegligible thickness in origami This technique is suitable for capturing thick origami or origamiinspired systems with blocked volume. References [4] and [190]. Left figure from Ref. [190]. Figure reproduced with permission from American Society of Mechanical Engineers ASME (2020).

structures and has been widely used in previous studies [19,21,24,26]. These strained (compliant) creases can be made with active materials such as shape memory polymers [133,134], hydrogels [19,24], shape memory alloys [18], light activated polymers, and others [25,26]. The smooth fold model can be used to study the folding behavior of this type of thick origami [103,104] because it can capture the widths of creases explicitly. Because the mechanical characteristics of the compliant creases (e.g., their bending stiffness) can affect the behavior of compliant crease origami systems significantly, it is more common to simulate these systems with mechanics-based simulation techniques. For example, both the compliant crease bar and hinge model [135,136] and finite element (FE) model [4] were used to simulate origami of this type. We will discuss these models when introducing mechanics-based simulations in Sec. 4 and multiphysics simulations in Sec. 5.

#### 4 Mechanics-Based Simulations

In this section, we introduce mechanics-based simulations for origami systems. The first step in creating a mechanics based simulation is to formulate a model that represents the origami structure and its internal properties. Figure 12(a) provides an illustrative example, where the single fold origami is represented using a point mass connected to an extensional spring (for panel stretching) and a linear-elastic rotational spring (for crease bending).

These mechanics-based models can then be used to simulate the physical behaviors of the origami due to applied loading, selffolding, or other external effects. The physical behaviors can be broadly separated into static or dynamic responses. In a static process, the kinetic energy of the system is assumed to be negligible. The goal is to solve for the deformed configuration  $\mathbf{x}$  under applied loading (or self-folding) to where the system is in equilibrium. This case usually forms a boundary value problem (BVP) where the internal forces (the Jacobian of the internal strain energy U) are equal to the external applied loads:  $\nabla_{\mathbf{x}}U(\mathbf{x}) = \mathbf{F}_{\mathbf{ext}}$ . These BVPs can be solved using various nonlinear BVP solvers (implicit solvers). Figure 12(d) demonstrates how typical nonlinear BVP solvers break the target load into small increments of load  $(\delta F_{ext})$ . Within each increment, the deformed state is iteratively updated to minimize error so that the solver can find the real solution (following the zig-zag curves in Fig. 12(d) to find the ground truth curve).

For dynamic behavior, the deformations occur rapidly, the kinetic energy of the system is no longer negligible, and we solve for the origami motions over time. Solving for the dynamic behaviors usually forms an initial value problem (IVP) (see Fig. 12(e)). The numerical integration methods previously introduced for kinematic simulations can also be used to solve these IVPs. These are explicit solution methods because they do not have iterative loops within their formulations (see Fig. 12(e)), which makes them faster than implicit methods per incremental step. However, because no iterative loops are used to minimize error, the numerical errors can accumulate over time. The accumulation of error limits the step length ( $\delta t$ ) of explicit methods, so these methods need to take large number of small steps for convergence and for achieving reasonable fidelity. Overall, this large number of steps typically makes solving dynamic simulations with explicit solvers

more time consuming when compared to solving static problems with implicit solvers. Technically, IVP can also be solved using implicit methods [137,138]. However, we will skip implicit methods for IVPs because they are not used widely for origami simulation.

A quasi-static simulation is a dynamic simulation with a slow loading rate, so that the kinetic energy is insignificant and instead the structural response is governed only by the static behaviors. A quasi-static simulation is useful when simulating origami with contact related behaviors such as the graded stiffness studied in Ref. [139].

In the remainder of this section, we introduce mechanics-based origami simulations and focus on the models to represent origami structures (i.e., part (a) of Fig. 12). After constructing the origami model, applying implicit or explicit solvers to run the simulation follows common procedures of mechanical analysis. A summary of different implicit solvers can be found in the work by Leon et al. [140] and common explicit solvers for dynamics simulations can be found in structural dynamics text books [137,138]. This section is arranged as follows: First, we introduce rigid panel models for kinematic analysis, which can be seen as the transition from kinematics-based simulations to mechanics-based simulations. Next, we present bar and hinge models and plate theory based models, which are two popular reduced-order models for origami structures. We then introduce FE models for origami structures that can offer high fidelity results. Following the discussion of these models, we proposed building hybrid reduced-order models for origami systems, and discuss how contact behaviors can be captured for origami systems. Table 2 summarizes the simulations and the models we cover in this section.

**4.1 Rigid Panel Models.** The close connection between kinematic and mechanical simulations of origami can be illustrated by considering the folding stiffness of a Miura-ori structure; see Fig. 13. After assigning rotational springs to the folding creases of this

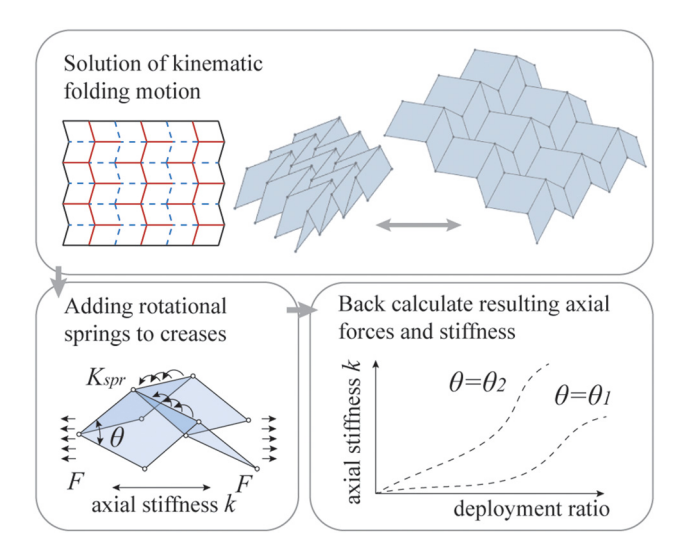


Fig. 13 Using kinematic simulations to capture simple mechanical responses

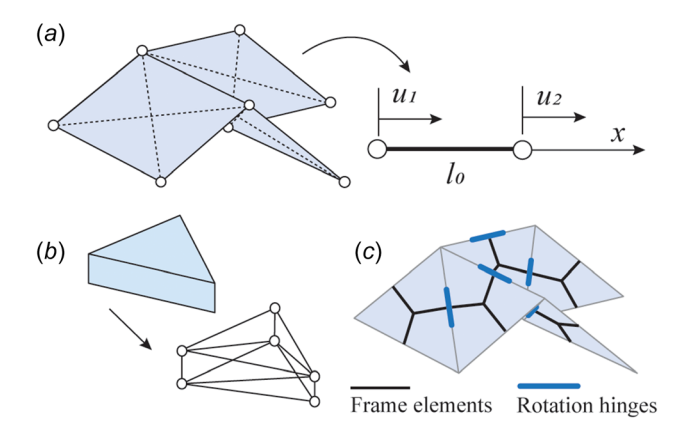


Fig. 14 Rigid panel models for kinematic studies. (a) Rigid bar models; (b) rigid truss model for thick origami; and (c) rigid frame models.

origami pattern, the internal hinge moments and total elastic potential energy at any rigid-foldable configuration can be calculated using the kinematics given in Eqs. (12)–(15). From the elastic potential energy, the force–displacement response (and thus stiffness) of the fold pattern can be found using Castigliano's theorem. This approach allows for rapid parametric studies, but is only suitable for obtaining simple mechanical behavior of rigid-foldable origami with known kinematics [60,62,78,79,82].

Next, we introduce rigid panel models for origami structures. These models can be seen as transitional models that lie between kinematic simulations and mechanical simulations. They usually use rigid truss elements or frame elements to represent the panels of origami structures and can capture the folding kinematics of origami.

Figure 14(a) demonstrates a technique to represent rigid origami panels using rigid bar elements and pin-joints. To analyze the kinematic folding motions of the origami system, one can study the compatibility matrix  $C_{\rm bar}$  of the rigid bar system

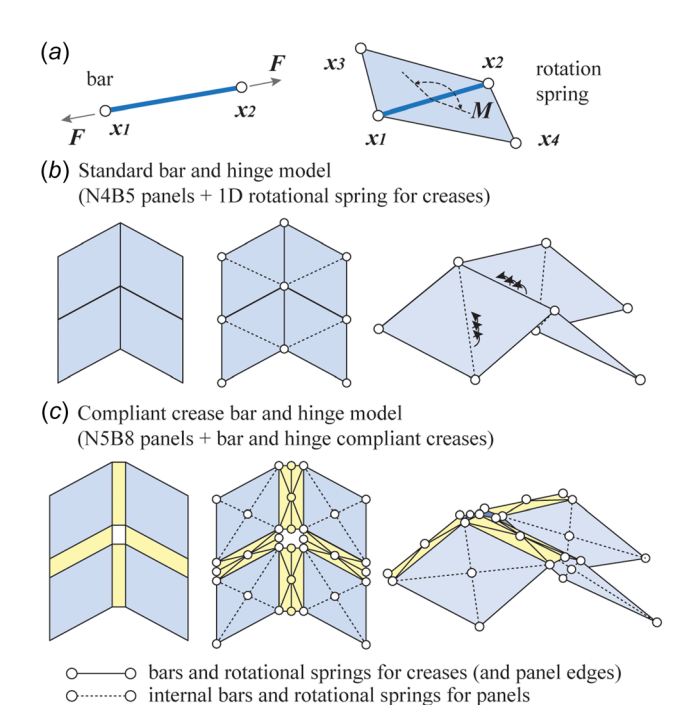


Fig. 15 (a) The bar element and the rotational spring element; (b) standard bar and hinge model for representing origami; and (c) compliant crease bar and hinge model for representing origami

[61,141,142]. This compatibility matrix relates the nodal deformation of the structure  ${\bf u}$  to the internal member strains  ${\bf e}$  as

$$C_{bar}(\mathbf{u})\,\mathbf{u} = \mathbf{e} \tag{23}$$

We use the 1D bar shown on Fig. 14(a) to demonstrate how this compatibility matrix can be calculated. The engineering strain of this bar is expressed as  $e = (u_2 - u_1)/l$ . Reorganizing the equation gives  $e = [-1/l, 1/l][u_1, u_2]^T$  so the compatibility matrix is [-1/l, 1/l]. More systematic ways of deriving the compatibility matrix for complex structures can be found in structural analysis textbooks [191] or in the following papers [61,141,142]. This compatibility matrix also relates the velocity of bar strains with respect to the velocity of nodal displacements

$$C_{bar}(\mathbf{u})\,\dot{\mathbf{u}} = \dot{\mathbf{e}} \tag{24}$$

Assuming the panel is rigid, there would be no bar strains throughout the kinematic motion which is equivalent to

$$\mathbf{C_{bar}\dot{u}} = 0 \tag{25}$$

This Eq. (25) is similar to Eq. (19) introduced in Subsec. 3.4. Both of these equations form an ODE and can be solved using the numerical integration methods and explicit solvers. The  $C_{\rm bar}$  matrix demonstrated in Eq. (25) plays the same role as the C matrix in Eq. (19). However, the derivation of  $C_{\rm bar}$  is directly obtained by solving the compatibility matrix rather than taking a kinematic approach. On top of the rigid bar constraint, rotational springs can be added to capture mechanical loading and other stiffness properties [61].

In addition to capturing thin origami panels, rigid truss models can also be used to capture the kinematic motion of thick origami panels [142]. In this formulation, a set of truss-based pyramids are used to represent the thick and rigid origami panels (see Fig. 14(b)). Although the current model has not been used to study deformable thick panels, this model can be extended for such studies in the future.

Hayakawa et al. introduced a related frame element based alternative for origami kinematic simulation [143,144] (Fig. 14(c)). Here, triangulated panels of the origami are represented using three frame elements that are rigidly connected at the panel center, and the folding creases are represented by rotational hinges at the crease line where two panels connect. If the frame elements remain rigid during the deformation, the system will preserve the kinematics of the rigid and thin origami. After deriving the compatibility matrix, numerical integration allows to track

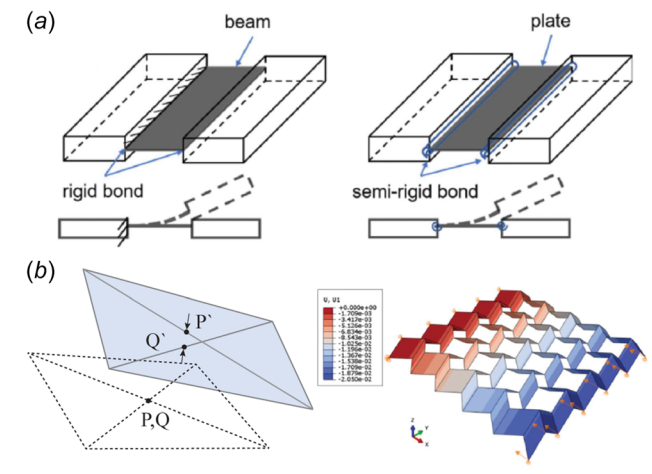


Fig. 16 Using plate theory based models to capture origami systems. (a) [167] reproduced with permission from Elsevier (2021); and (b) right [168] reproduced with permission from Springer Nature (2021).

kinematically admissible motions. The work by Hayakawa et al. also demonstrated that this model can be used for inverse design of origami patterns that fit arbitrary surfaces [143,144].

**4.2 Bar and Hinge Models.** The bar and hinge model has become a widely used reduced-order mechanical model for representing origami systems [28,62,151,152]. The model is sometimes referred to as the truss-based mechanism model [149,150,155] or the pin-jointed bar framework [61], but here, will use the name *bar and hinge model* because it is an expressive name (directly pointing to the two elements involved).

The model represents an origami using bar elements and rotational spring elements (hinges with rotational stiffness) as shown in Fig. 15(a). The bar elements are extensional springs in 3D space that can capture the stretching and shearing of origami panels (and creases). On the other hand, the rotational spring elements are rotating hinges with stiffness that can capture the crease folding or panel bending. The strain energy stored within the entire origami system can be expressed as

$$U = \sum_{i=1}^{N_{\text{bar}}} U_{\text{bar},i} + \sum_{j=1}^{N_{\text{spr}}} U_{\text{spr},j}$$
 (26)

where  $U_{\mathrm{bar},i}$  represents the strain energy in bar i and the  $U_{\mathrm{spr},j}$  gives the strain energy of rotational spring j. The simplest bar element is a linear spring and can be expressed as

$$U_{\text{bar},i} = \frac{1}{2} \frac{E_i A_i}{l_{0,i}} \left( |\mathbf{x}_1 - \mathbf{x}_2| - l_{0,i} \right)^2$$
 (27)

where  $E_i$  is the Young's modulus,  $A_i$  is the bar area,  $\mathbf{x}_1$  and  $\mathbf{x}_2$  are the nodal coordinates, and  $l_{0,i}$  is the original length of the bar. Many studies use this linear elastic bar formulation because it is simple and easy to derive [43,136,149,150,152,156]. More advanced hyper-elastic formulations are also available for deriving the total potential of the bar element [63,192,193]. Similarly, the linear elastic rotational spring model is the simplest hinge element and it can be expressed as

$$U_{\text{spr,i}}(\mathbf{x}_{1},\mathbf{x}_{2},\mathbf{x}_{3},\mathbf{x}_{4})$$

$$= \frac{1}{2} \mathbf{K}_{\text{spr,i}} (\phi(\mathbf{x}_{1},\mathbf{x}_{2},\mathbf{x}_{3},\mathbf{x}_{4}) - \phi_{0})^{2}$$
(28)

where  $K_{spr,i}$  is the spring stiffness,  $x_1$  to  $x_4$  are the nodal coordinates, and  $\phi_0$  is the stress free dihedral angle of the fold. The current dihedral angle can be calculated using the current nodal coordinates of the four nodes adjacent to the fold (see Fig. 15(a)), and detailed calculations of this function  $\phi$  can be found in [63,149,168]. Most existing studies use this linear elastic rotational spring formulation [43,136,149–153,156].

There are different ways of meshing an origami structure using the bar elements and the rotational spring elements. The N4B5 model [61,63] and the N5B8 model [145,193] are two common models for a quad origami panel. The N4B5 model represents a quad panel with four nodes and 5 bar elements (see Fig. 15(b)). This N4B5 model can capture the bending behavior across one diagonal axis of the quad panel but produces a skewed deformation under in-plane axial loading. In order to avoid this skewed deformation, the N5B8 model (see Fig. 15(c)) was proposed by Filipov et al. in Ref. [145]. This panel model contains five nodes and 8 bars. With the additional bars, it produces a more accurate deformation under the applied axial loading and can capture bending across both diagonals of the panel. In addition to these models for quad based origami, the generalized N4B5 and generalized N5B8 models are also proposed for panels with arbitrary number of edges by Liu and Paulino in Ref. [193]. Finally, explicit derivations for trapezoidal and hexagonal panels are provided by Redoutey et al. in Ref. [194].

In a standard bar and hinge model, the folding creases of the origami structure are represented with individual rotational springs [28,43,62,145–153]. In this formulation, the folding creases are simplified as lines with no width (see Fig. 15(b)). This type of model can capture the crease folding, panel bending, panel stretching, and panel shearing deformations. However, the model cannot capture possible extensional and torsional crease motions in compliant creases.

More recently, the bar and hinge model has been extended to capture compliant creases within active origami [135,136]. In this formulation, the compliant creases are represented using seven nodes, 12 bars, and eight rotational springs (see Fig. 15(c)). Using compliant crease bar and hinge model can further capture the extensional strain energy in folding creases, which is necessary for capturing some bistable behaviors in origami structures [135,136].

There are three main approaches to assigning stiffness parameters (bar areas and rotational spring stiffness) when using bar and hinge models. First, it is possible to assign fictitious values to the bar area and the rotational spring stiffness [195]. This technique can be used when studying the algorithmic properties of origami simulations (such as studying parallel computation or convergence properties), where we are less interested in predicting the exact physical origami behaviors. Second, we can derive the stiffness parameters by matching the stiffness of a bar and hinge model to that of a theoretical plate model [136,145,193]. Because these derivations tend to be based on a small-deformation assumption, the generated stiffness parameters can produce mechanical behaviors that are stiffer than physical experiments where large deformations such as panel buckling occur. Finally, it is possible to assign the bar area and the rotational spring stiffness by doing curve fitting using experiments [196]. This approach tends to produce a more accurate prediction of the origami stiffness because curve fitting can artificially account for large panel deformations. In other words, using curve fitting is similar to using the secant stiffness, while matching with theoretical plates is similar to using the initial tangent stiffness.

Simulating origami mechanical behaviors using bar and hinge models and static nonlinear solvers has become popular because these models have a simple formulation and are computationally efficient. This simulation technique can capture the global response of origami structures and allows richer deformation to be simulated when compared to kinematics-based simulations. So far, bar and hinge model simulation techniques have been successfully used for studying the bistability and multistability in origami hypars [146,148] and Kresling patterns [63,153,154,156], capturing the folding motions of tubular origami [28,152], studying the behaviors of compliant crease origami [135,136], designing origami metamaterials [62,197], optimizing the performance of origami patterns [150,157], studying the influence of origami defects [147], and more. However, the bar and hinge model cannot capture localized behaviors such as crease buckling, panel buckling, stress concentration, and local material plasticity in the origami structures.

The bar and hinge model can also be used to study the dynamics of origami systems. To do that, one needs to use a particle bar and hinge formulation. This formulation captures the mass of origami by assigning "particle" mass to the nodes of the origami models [159,161–163]. The velocity and acceleration of the origami are also stored at these mass nodes [159,161–163]. The dynamic motions of the origami structure can be solved using explicit solvers such as those introduced in Refs. [137,138, and 198]. This model is used to study the folding dynamics of various origami structures including Miura tubes [159], Miura sheets [165], waterbomb tubes [163], and Ron-Resch patterns [161]. This model can also be used to study "chaotic" type dynamic folding behaviors in origami [199–201].

**4.3 Plate Theory-Based Models.** Because origami tends to have planar characteristics, plate theories can be used for

representing both compliant creases and deformable origami panels. In the work by Zhang et al., a theoretical plate model for capturing the mechanics of compliant creases is proposed [167]. In their work, additional rotational springs were added at the connection between the origami panels and the compliant creases so that richer deformations could be enabled (Fig. 16(a)). In a more recent work by Zhang [166], this advanced plate theory-based model is incorporated into a bar and hinge model to capture the behaviors of an entire origami pattern.

Plate theory-based models can also be used for capturing the behavior of origami panels. Hu et al. [168] created a user defined quad element in ABAQUS to capture the small-deformation behaviors of origami plates. In their approach, the quad element is designed such that it can capture the panel bending using the separation distance between the center points of the two straight lines that connect opposite corners of the quad panel (Fig. 16(b)). The potential of this quad element is calculated as

$$U = \frac{D^e}{2} (\Delta w)^2 = \frac{D^e}{2} (\mathbf{u_P} - \mathbf{u_Q})^2$$
 (29)

This formulation is derived with assumed small curvature deformation [168]. In the equation, the term  $D^e$  is a modified bending rigidity of the plate and the subtraction  $\mathbf{u_P} - \mathbf{u_Q}$  obtains the distance between point P' and Q' (see Fig. 16(b)). Their work demonstrates that if the panel deformation is governed by small-strain bending, the model can capture the origami behaviors rapidly. Similar approaches were also used by the authors to study the inverse design of freeform origami systems [202]. In addition to this formulation, the study by Soleimani et al. [169] derived a plate theory-based panel model using the first order shear deformation theory.

Using plate theory-based panel models and crease models can be thought of as using FE models with coarse meshes. These plate theory-based models can provide a lower fidelity but more computationally efficient approaches to capture the behaviors of origami compared to the use of FE models. However, plate theory-based origami models cannot capture extreme local buckling and kinking because these models are derived with strict assumptions on the deformation shapes.

**4.4 Finite Element Models.** Using FE models is another popular way for representing origami-inspired engineering structures. FE models provide approaches to capture the complicated local behaviors (such as local buckling and stress concentration

[174,180,181]) and material nonlinearity (such as plasticity [177,178]) in origami structures. In addition, most commercial FE packages also provide automated internal static and dynamic solvers for users to choose from. In this subsection, we focus on how FE models are used for studying the mechanical behaviors of origami systems such as stiffness under static loading and energy absorption under dynamic loading. In addition to these purely mechanical studies, FE models are also widely used for capturing multiphysical behaviors of origami systems, and this topic will be discuss in Sec. 5.

One way to capture origami using FE is to represent the panels using shell elements and connect the panels using rotational springs or hinges [28,145,170,171] (see Fig. 17(a)). This approach is commonly used for studying the mechanical properties of origami sheet and tubular structures because it can capture the relatively soft creases in such systems. Filipov et al. have used this approach to study a reconfigurable tubular origami structure [170] and a stiff zig-zag origami tube [28]. Both the load bearing capacity and the eigen properties of origami tubes are investigated [28,170]. A similar approach was used in work by Grey et al. [171] to study the deployment process of Miura-ori tubes with crease actuation.

Another way of capturing origami structures using FE models is to connect the shell element panels with fixed and rigid fold lines (see Fig. 17(b)). This formulation is suitable for studying the behaviors of origami-inspired devices such as metamaterials, crash boxes, and sandwich cores. These origami-inspired devices are not fabricated for deployment. Instead, these devices are overconstrained and used as a single block of material with fixed creases. First, this FE model setup was used for exploring the static response [176,178] and the dynamic response [177] of origami metamaterials. For example, Yuan et al. show one origami inspired metamaterial that can produce programmable stiffness for various engineering applications [176]. In addition, this FE model setup has been used for analyzing origami crash boxes for energy absorption applications [183-186]. For instance, Wang and Zhou [184] use this approach to study the influence of imperfection sensitivity of origami crash boxes, and Xiang et al. [182] provide a detailed review on using origami-inspired structures for energy absorption. Finally, this FE setup can study the behaviors of origami sandwich cores. Heimbs et al. [180,181] use this FE formulation to capture the complex material failures such as delamination in origami cores, and Schenk et al. [179] used this approach to study the behavior of stacked Miura-ori sandwich beams for blast-resistance. In all of the above studies, the deployment of the origami structure is restricted and the systems are

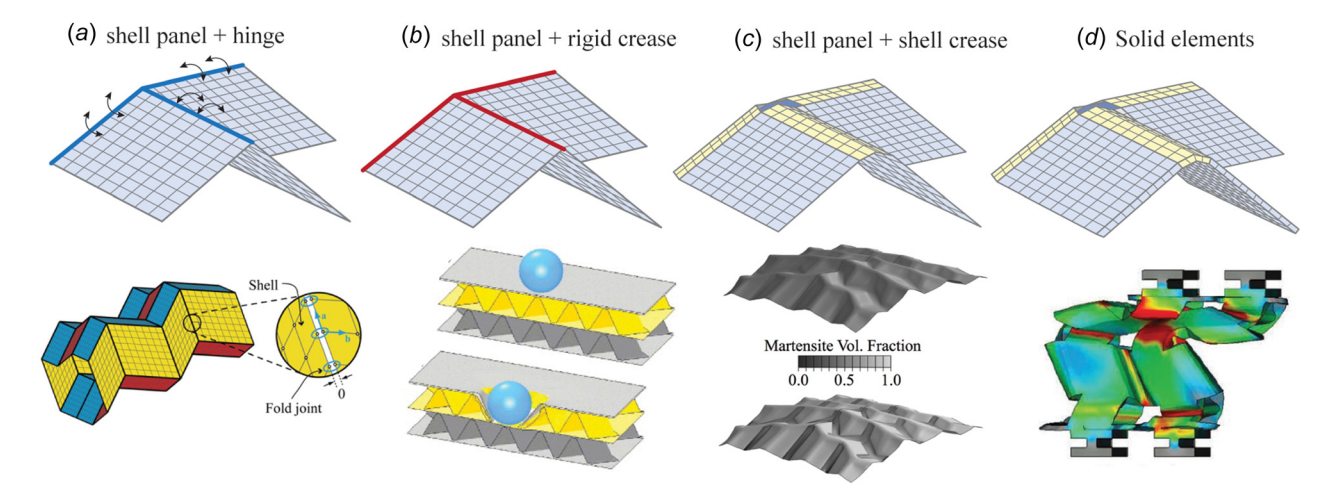


Fig. 17 Different types of FE models for origami structures. (a) Bottom [170] reproduced with permission from the Royal Society (2016); (b) bottom [181] reproduced with permission from Elsevier (2010); (c) bottom [189] reproduced with permission from American Society of Mechanical Engineers ASME (2016); and (d) bottom [4] reproduced with permission from John Wiley and Sons (2018).

kinematically over constrained. Typical deformation of these systems includes panel buckling and stretching, and the local crease deformations are not considered to be important for the global behaviors.

Compliant origami creases can also be captured using shell elements as shown in Fig. 17(c) [104,135,136,189]. In this approach, the geometry and stiffness of the compliant creases can be accurately captured using shell elements with fine meshes. Capturing the compliant creases explicitly can be important for many reasons. For example, it allows users to consider the active folding from plate-based bending actuators [189].

Finally, solid elements can also be used for representing origami-inspired systems [4,190]. In these cases, solid elements are used to properly capture the full system geometry of origami-inspired structures because the panel thickness is important. Using this approach is computationally expensive because fine meshes across the thickness of origami panels are needed to capture the accurate panel bending behavior. Thus, solid elements are usually not used for representing origami systems unless explicitly capturing the thickness is of essential importance.

One major reason behind the popularity of using FE models for origami structures is the existence of commercially available software programs such as ABAQUS [139,176,183], ANSYS [180,187], and LS-DYNA [180,181]. These commercially available programs provide a wide variety of material models and element types, and allow researchers to perform static loading, quasi-static loading, or dynamic loading using standardized procedures through convenient user interfaces. The FE models also capture local structural responses such as stress concentration and local buckling [173,174,180,181], which is otherwise difficult to capture with reduced-order models. However, building FE models and running the analyses is time-consuming, especially if the origami is made with nonrepetitive base patterns. Because of those difficulties, most of the studies covered in this subsection were based on simple patterns such as the Miura-ori pattern. Transforming "freeform" origami designs into executable FE software programs in a stream-lined manner is still a difficult task to be resolved. Another limitation of using FE model is that an FE model acts like a black box. Many scientific explorations and theoretical developments still favor the use of reduced-order models because they can reveal the underlying theoretical behaviors (as will be discussed further in Sec. 7).

4.5 Rethinking Reduced-Order Mechanical Models for Origami: Hybrid Formulations. In this subsection, we take a step back and provide a holistic discussion on the formulation of reduced-order mechanical models for origami systems. Unlike kinematics-based simulations for origami systems, mechanicsbased simulations allow users to combine different panel models and crease models to assemble new "element-based" formulations. We can think of the formulation of a mechanical model as "gluing" different "elements" at the nodes of the origami structure. These different elements will generate the relationships between internal forces and nodal deformations needed to capture the folding and loading behaviors of origami systems. When FE models are used for representing origami systems, we are already modeling the origami by grouping different panel models and different crease models. The same perspective can be applied to the reduced-order origami models for creating new hybrid formulations. Figure 18 demonstrates how combining different simplified origami panel models and crease models can potentially create new reduced-order models. The key of achieving this combination is to ensure that the panel models have identical boundary setups (number of nodes and number of DOF per node) as the crease models.

All models demonstrated in Fig. 18 were discussed previously except the spring-based models for creases, which we will now briefly discuss. The simplest way of capturing the mechanical behavior of origami creases is to use a single spring element. In addition to the common rotational springs for capturing crease folding motions [28,63,149,150], other deformations between the two panels can also be captured using spring elements with different forms. In general, there are six different forms of relative deformations between the two panels as shown in the bottom left box of Fig. 18. In many situations, we do not need all six forms of deformations to capture the accurate global mechanical behaviors of origami systems. For example, studying the Poisson's effects or the stretching stiffness of Miura sheet only requires using rotational springs for the folding motion [61,62] and capturing a bistable origami cone can be accomplished with rotational springs and extensional springs [203]. There are also models including all six forms of springs such as the one proposed by Soleimani et al. [169]. These six forms of springs provide a useful tool to model the behaviors of lamina emergent mechanism (LEM) type joints for origami, which is a novel technique for building thick origami

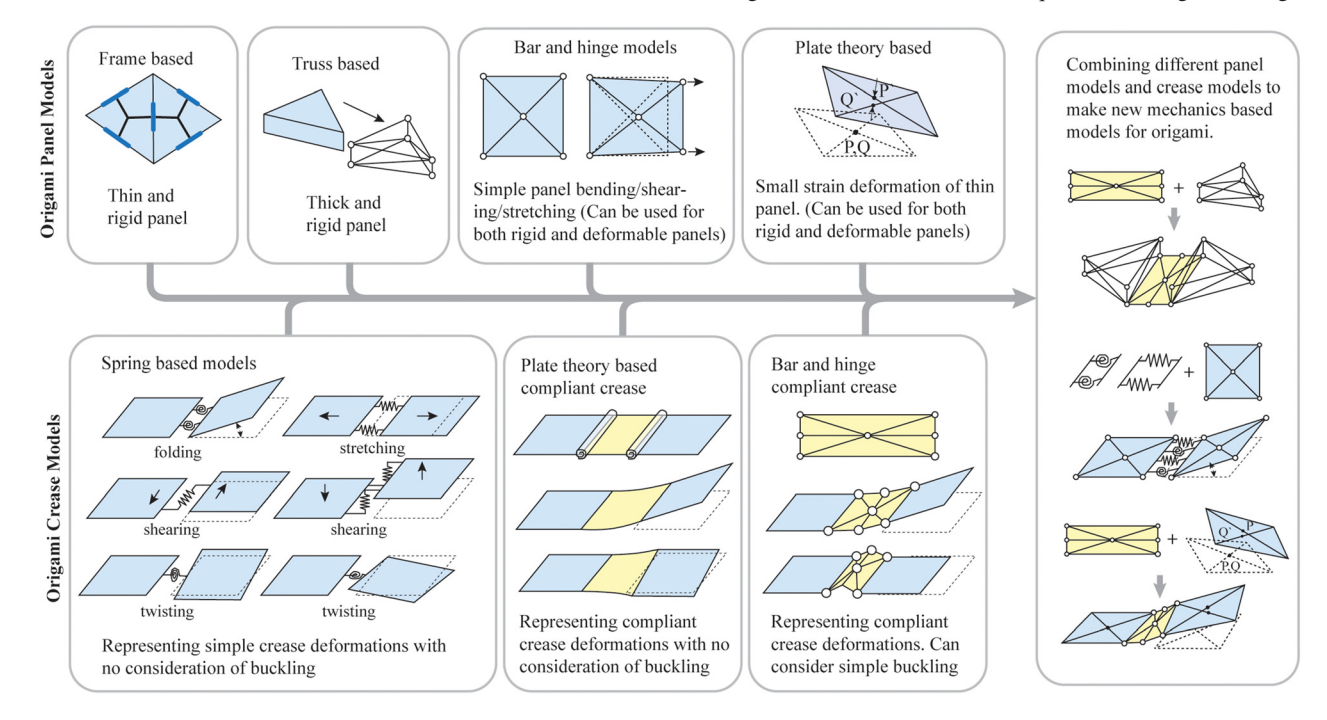


Fig. 18 Different types of mechanical models for origami panels and creases could be combined to create hybrid models

systems (introduced in Sec. 3.7). The work by Delimont et al. provides a summary of different LEM joints and equations for calculating the corresponding spring stiffness [132]. Spring-based models are appropriate for capturing linear origami crease behaviors or behaviors with small deformations. However, the models are not suitable for capturing the distributed width of compliant creases or for capturing localized behaviors such as buckling of creases.

Considering the variety of different panel and crease models, one can create new origami models tailored for specific origami systems by combining appropriate models (Fig. 18). In this way, one can create a hybrid origami model that inherits both the capabilities from the selected crease model and the selected panel model. For example, the truss-based thick panel model [142] can be grouped with the bar and hinge compliant crease model [135,136] to capture the behaviors of origami systems with strained creases and thick panels. Alternatively, the plate theory based panels [168,169] could be grouped with spring based creases to capture deformable origami with small-strain plate bending and linear crease deformations.

Some of the current implementation packages for origami simulation already allow users to choose between different combinations. For example, the bar and hinge MERLIN package allows users to switch between the N4B5 and N5B8 panel models [193,204] and the bar and hinge swomps package allows users to switch between the spring based creases and compliant creases [64,205]. However, the variability provided with current packages is still limited. Future studies on reduced-order mechanical models for origami systems can explore the potential of generating a more unified formulation to incorporate different panel models and crease models. In addition, future implementations can expand built-in panel models and crease models so that users can create more on-demand combinations for the specific origami that they are working with.

**4.6** Capturing Panel Contact. One fundamental limitation in the kinematics-based simulations of origami is that panel contact

within origami systems cannot be easily captured (see Fig. 9). However, capturing the occurrence and behavior of panel contact can be important for studying origami-inspired metamaterials or crash boxes as shown in Refs. [176], [178], and [183]. Thus, in this subsection, we briefly discuss how mechanics-based simulation techniques can capture the panel contact within origami systems. We discuss panel contact models for static simulations and dynamic simulations separately because they tend to have different formulations and characteristics.

To prevent the origami panels from penetrating each other in a static simulation, the internal strain energy (potential) of the origami structure needs to be adjusted. This can be achieved by changing the strain energy formulation of the rotational springs. In the work by Liu and Paulino [63,192], a piecewise penalty function is added to the strain energy of the rotational springs. This additional penalty function gives a large stiffness when the crease folds toward 180 deg so that the crease is prevented from over-folding (see Fig. 19(a)). Similarly, a slightly different but continuous strain energy formulation of rotational springs is provided by Gillman et al. [149,150] (see Fig. 19(b)). This continuous form can also avoid local penetration.

However, these formulations only prevent panels from penetrating each other locally (the two panels need to share a common hinge). A more thorough penetration prevention technique was developed in Ref. [158]. In their work, the penalty function for panel contact is developed based on the distance between a contacting triangle panel and a contacting node. This technique can prevent panel penetration globally and the contacting panels do not need to share a common crease. Figure 19(c) demonstrates a sample application of this model, where contact results in a stiffness jump between two separate but interlocked origami strips. This model also provides the capability to capture thickness in origami within a mechanical simulation [158] (see Fig. 19(d)).

Both the local and the global panel contact models introduced above have a potential based formulation. That is to say, the panel contact forces can be determined based on the current configuration of the origami (without the history of prior configurations).

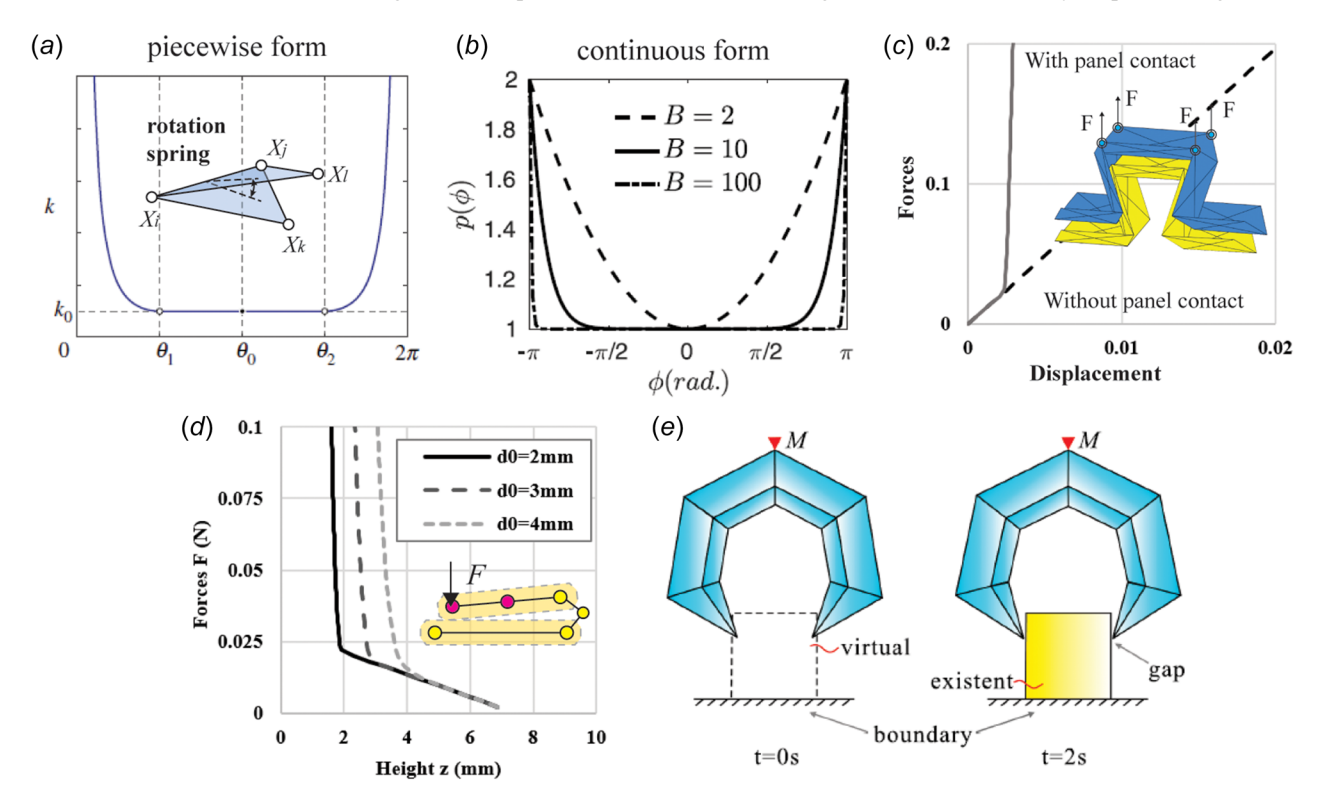


Fig. 19 Panel contact and prevention of panel penetration in origami simulation. (a) [63] reproduced with permission from the Royal Society (2017); (b) [149] reproduced with permission from Elsevier (2018); (c) and (d) [158] reproduced with permission from the authors; and (e) [164] reproduced with permission from Elsevier (2021).

Because these are potential-based formulations, the contact forces within these models are conservative (there is no energy dissipation). One advantage of using these contact models is that they are fast to solve. This is because these static contact models form a BVP that can be solved statically using implicit solution methods. However, these potential based contact models cannot capture frictional forces. To resolve this limitation, one needs to construct IVPs and use dynamic-based (or quasi-static based) simulation techniques such as those proposed in the work by Dong and Yu [164] (see Fig. 19(e)). In their model, the panel contact forces are not only calculated using the current origami configuration, but are also calculated using the velocity of origami motion (see Eq. (14) in Ref. [164]). This panel contact model forms an IVP because calculating the velocity of origami motion needs to use the origami configurations from previous steps. Solving these dynamic contact models are more time-consuming because they need to use the explicit dynamic solution methods.

In addition to using the above-mentioned reduced-order models for capturing contact, commercial FE simulation programs can also be used to study contact-related origami behaviors. For example, Ma et al. studied the quasi-static loading of an origamiinspired structure with graded stiffness [139] and an origami crash box for energy absorption [206]. Similarly, Heimbs et al. studied dynamic impact loading [181] and quasi-static loading [180] of origami sandwich fold cores using FE simulations. Usually, even when exploring static contact behaviors in origami, a dynamic performed simulation (in a quasi-static manner) is [139,183–185,188]. The reasoning is that explicit solvers in FE simulation packages often provide better contact models and contact searching algorithms [207-209].

## 5 Multi-Physics-Based Simulations

Recently, there has been an increased need to analyze the multiphysics-based active folding and other nonmechanical

properties of origami-inspired systems such as thermally active folding [21], magnetic active folding [210], electromagnetic properties of origami-inspired systems [38], drag force of origami surfaces in submerged environments [107], and thermal expansion properties of origami [9]. Figure 20 (a) gives a general flowchart for analyzing origami using multiphysics-based simulations. Generally speaking, there are two processes that involve the use of multiphysics simulations and they are: simulation of the actuation for active folding and the simulation of nonmechanical properties. In this section, we discuss these two aspects of origami multiphysics.

Traditionally, origami artists fold an origami using their hands and their craftsmanship. But nowadays, origami engineers take other approaches and fold origami-inspired engineering systems using active materials or responsive systems. For example, origami-inspired systems can be folded using active hydrogels [19,20,24], metallic morphs with residual stresses [25,26,211,212], shape memory polymers [13,14,134], shape memory alloys [18,189,213], electrothermal actuators [21,64], active magnetic systems [210,214–216]. The folding motions generated using these actuation mechanisms have a multiphysical nature, and thus, multiphysics-based simulations are needed.

The multiphysics-based actuation can act on the origami through two major types of action: by triggering crease folding or by triggering globally applied forces. In the first type, the applied stimuli first trigger the material in the crease region to develop strains and stresses. The strains and stresses then force the crease to bend and transform the origami into a folded geometry. Most active origami systems achieve shape morphing using this form of actuation. When determining the relationship between the applied stimuli and the crease folding, both experiment-based and simulation-based approaches can be used. For example, in the work by Leong et al. [26,211], experiments were used to determine the folding angle given the heating or other applied stimuli. On the other hand, in the work by Zhu and Filipov [64], a bar and

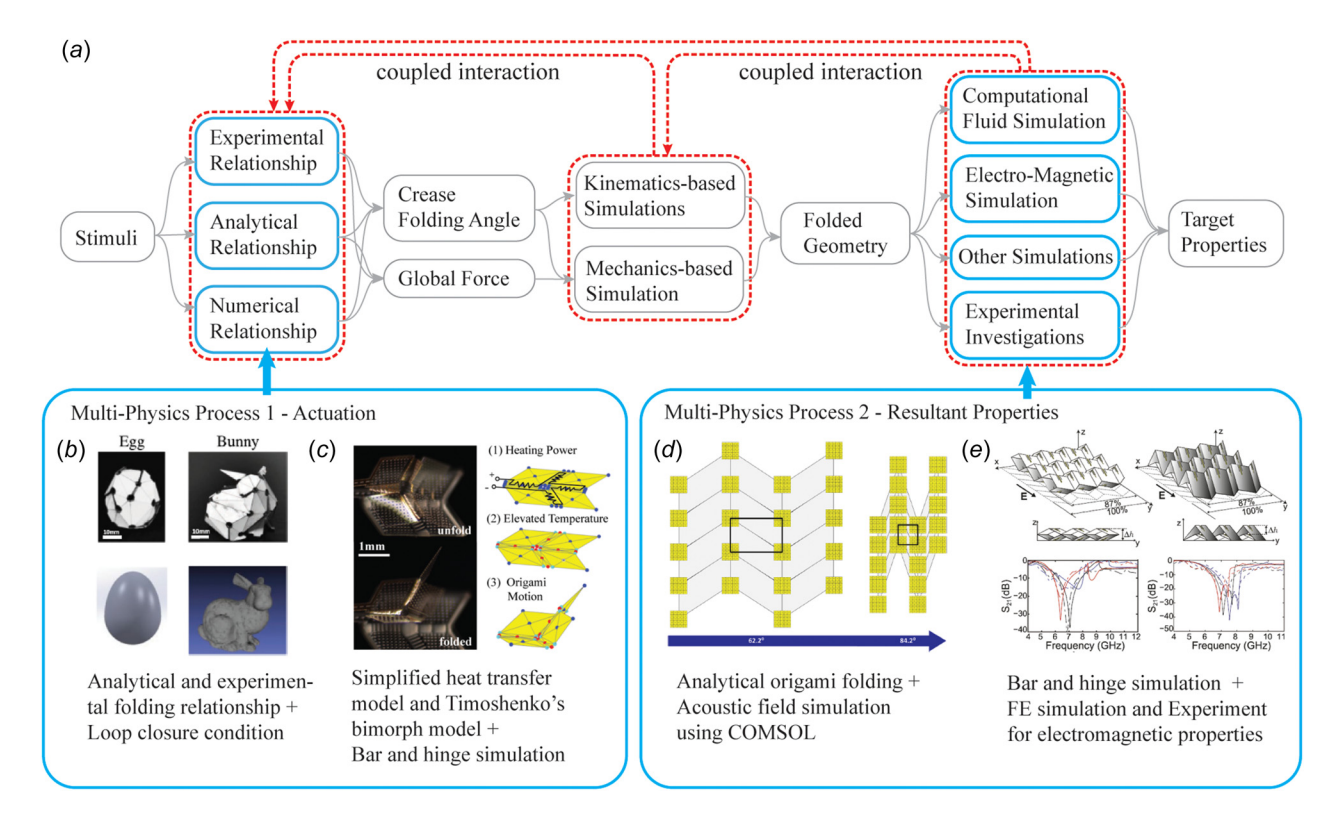


Fig. 20 Multiphysics simulation of origami captures the actuation, the resultant properties, and the potential coupling (indicated with dashed lines) between these behaviors. (b) [13] reproduced with permission from the Institute of Electrical and Electronics Engineers IEEE (2018); (c) [64] reproduced with permission from the authors; (d) [65] reproduced with permission from AIP Publishing; and (e) [39] reproduced under CC BY-NC-ND license.

Table 3 A summary of available simulation packages for origami structures

Package Formulation Reference and links

If the input pattern is rigidly flat foldable, the pro-

generate the folded geometry of the origami. The

brute-force approach.

gram will use reflection based simulation to directly

program then calculates the panel sequence using a

The Rigid folding simulator use Euler's integration

to track the folding trajectory that complies with the

loop closure constraint. The Origamizer can fit any

triangulated 3D surface using origami with a tuck-

folding technique. The Freeform origami is based on the Rigid folding simulator and allows users to drag vertices of an origami for creating new origami

Flat-foldable origami ORIPA



Loop closure constraint

Rigid folding simulator and Origamizer and Freeform origami





Kinematic compliant crease simulation

Smooth fold simulation







Bar and hinge simulations

MERLIN



Origami Simulator

OMTO and nonlinear truss



This is a MATLAB based implementation of the smooth fold simulation. This kinematics-based simulation can capture the compliant crease geometry in origami structures.

MERLIN is a MATLAB based implementation of the standard bar and hinge model. MERLIN implements the N4B5 panel formulation and solves the mechanical behavior using a modified generalized displacement control method. A newer version of the code provides the generalized N4B5 and N5B8 panel models.

This is a GPU accelerated version of the standard bar and hinge models. The simulation is based on the formulation demonstrated in Ref. [61] and the

pattern editing is based on Ref. [91].

These two packages implement the standard bar and hinge model proposed in Refs. [149] and [150], and can perform topological optimization to generate

origami patterns for certain functions.

This is an object oriented MATLAB implementation of the bar and hinge simulation capable of simulating compliant creases, global interpanel contact, and electrothermal actuation in active origami. The program supports five loading solvers and can treat the origami with an arbitrary number and sequence of

This a physics engine developed for Rhino and Grasshopper. The package can be used to simulate origami system and was used for capturing magnetic active origami in Ref. [210].

This is a Grasshopper plugin for Rhino. The folding simulation and form finding is based on the Freeform Origami. The package can also simulate thickness in origami systems.

References [57], [68], and [119]. Package found in Ref. [68]. Left figure from Ref. [68]. Figure reproduced with permission from the authors.

References [56], [91], [93], [97], [230], and [231] Packages found in Refs. [97], [230], and [231]. Left figures from Refs. [97,230]. Figures reproduced with permission from the authors.

References [103] and [104] Package found in Ref. [103] Left figure from Ref. [103]. Figure reproduced with permission from American Society of Mechanical Engineers ASME.

References [63], [192], [193], and [204] Package found in Ref. [204]. Left figure from Ref. [204]. Figure reproduced with permission from the authors.

References [195] and [232]. Package found in Ref. [232]. Left figure from Ref. [232]. Figure reproduced with permission from the authors.

Reference [149,150,233,234] Package found in [233,234]. Left figures from Refs. [233,234]. Figures reproduced with permissions from the authors.

References [64], [135], [136], [158], and [205]

authors.

Package found in Ref. [205]. Left figure from Ref.

[205]. Figure reproduced with permission from the

References [210], [219], and [220] Package found

in Ref. [219]. Left figure from Ref. [219]. Figure

reproduced with permission from the authors.

SWOMPS



Add-on and commercial tools

Kangaroo







loading steps.

References [91] and [235] Package found in Ref. [235]. Left figure from Ref. [235]. Figure reproduced with permissions from the authors.









Commonly used commercial FE software programs include ANSYS, ABAQUS, LS-DYNA, COMSOL, and many others.

See Sec. 4.4 for details. Figure from Ref. [170] reproduced with permission from the Royal Society (2016)

Small strain plate



This model is implemented using user defined elements in ABAQUS for capturing origami panels. This plate model can capture the small-strain bending of panels.

Reference [168] Code found in the appendix of [168]. Figure from Ref. [168] reproduced with permission from Springer Nature (2021)

hinge model with heat transfer and a Timoshenko's bimaterial morph model are used to solve the crease temperature and the folding motion from the applied heating power [217]. Similarly, the work by Deng et al. developed a simplified model to capture the active folding in a prestressed polystyrene film crease actuator [218]. In general, active material-based crease folding tends to rely on using compliant creases with distributed crease regions and bimaterial layers. Therefore, the behavior of this active origami can be better captured using models such as the smooth fold model, the compliant crease bar and hinge model, or with FE models. The analysis of the bimaterial morph by Timoshenko [217] also provides a direct analytical solution to correlate material strains and the crease folding of active compliant creases.

Stimuli can also generate globally applied forces onto the origami to achieve the folding motion. Magnetically activated origami is one major genre of active origami using this form of actuation [210,214–216]. Magnetic forces acting on the origami structure can be calculated based on the orientation of the embedded magnets and the applied magnetic field. After calculating the magnetic forces, the folded configuration can be tracked using mechanics-based origami simulations. The work by Swaminathan et al. [210] provides a simulation technique that can capture these magnetic forces using the Kangaroo solver in Rhino [219,220]. Apart from magnetic systems, the forces could also be applied directly by connecting the passive origami system to an active supporting mechanism [221]. With such a system, the connected origami is deployed with forces from the supporting mechanism.

In addition to the actuation of active origami, multiphysics simulations are also needed to capture the nonmechanical properties of origami-inspired structures for design and for optimization. For example, origami-inspired structures have been used to create frequency selective surface (FSS) for filtering electromagnetic waves [38,39,222–225]. To analyze and design the performance of these FSS devices, electromagnetic simulation through commercial FE software programs such as ANSYS HFSS can be used [39]. Similar multiphysics-based simulations have been used to analyze origami-inspired engineering systems for acoustic wave manipulation [40,65,226–228], as thermal metamaterials [9], and for their drag forces in submerged environments [107].

Capturing variable multiphysics properties of origami systems usually requires using one simulation environment to capture the origami folding and another separate environment to capture the nonmechanical properties. In light of this complexity, it is important for future work on origami simulation to generate easy to use output formats that can easily interface with multiphysics-based simulation environments. A unified format such as the FOLD structure [229] could be useful for achieving trouble-free data transfer between different environments. However, additional information regarding the active folding systems, the compliant crease geometry, the material properties, the localized circuit

designs, and other origami properties of interest would need to be included. Another challenge of multiphysics simulation of origami is the coupling between the origami folding, the multiphysics actuation, and the nonmechanical performance (red dashed lines in Fig. 20). Simulating these coupled behavior and interactions requires passing information between different environments, which is still difficult to accomplish effectively. An alternative way to solve the coupling problem is to build reduced-order simulations within the same environment such as the simulation of electrothermal crease folding in Ref. [64] or the simulation of magnetically actuated origami in Ref. [210]. However, the capabilities of current reduced-order simulations are still limited so future work is needed.

#### 6 Available Simulation Packages

In this section, we introduce existing implementation packages for simulating origami systems and discuss their capabilities and potential application scenarios. Table 3 summarizes these packages.

First, Mitani's ORIPA [57,68] implements a reflection-based simulation for flat-foldable origami systems. The package directly solves the folded configuration using reflection-based theories and calculates the panel sequence using brute force enumeration. This package is one of the early computational tools developed for origami engineers. However, ORIPA cannot simulate the intermediate folding states, the folding process, or physical behaviors, which are all important for the analysis and design of engineering origami systems.

Next, the Rigid Folding Simulator, the Origamizer, and the Freeform Origami developed by Tachi share some similarities [97,230,231]. The Rigid Folding Simulator can capture the folding motion of origami systems-based on the loop closure constraint (Eq. (16)). Kinematically feasible folding motion is solved using numerical integration such as Euler's method (see Subsec. 3.4). The simulation package provides a rapid and effective implementation to study the kinematic folding of thin and rigid origami, providing one popular computational tools for simulating origami folding. Based on the rigid folding simulator, Origamizer [231] and Freeform Origami [97] were developed. Origamizer can design an origami to fit arbitrary 3D surfaces using a tuck folding technique, and Freeform origami allows users to design new origami patterns by directly editing existing tessellations. However, these three packages cannot capture compliant creases, panel deformations, mechanical properties, and other multiphysicsbased properties of origami.

The smooth fold simulation developed by Hernandez and his coworkers [103,104] is one of the first kinematic simulations to explicitly consider compliant creases within origami systems (see Subsec. 3.6). A MATLAB implementation was published as

electronic supplementary material in Ref. [103]. This package can capture the geometry and mechanics of compliant creases within active origami. However, because the simulation was developed based on rigid panel assumptions, this package cannot simulate behaviors related to panel deformations.

We further give a short description of existing implementations of the bar and hinge simulation. MERLIN [63,192,204] is a public implementation of the bar and hinge simulation that can track origami folding and mechanical deformations using a modified generalized displacement control method. The package is implemented in MATLAB and is based on the standard bar and hinge model formulation with the N4B5 panel model and the linear rotational spring based crease model. A newer version of the MERLIN package (MERLIN 2) [193] can further support the use of N5B8, generalized N4B5, and generalized N5B8 panel models, and provides useful functions to read OBJ format. These two packages are rapid and powerful tools for simulating origami folding and exploring mechanical properties such as stiffness, bistability, and multistability. The Origami Simulator [195,232] is a parallelized GPU-accelerated version of the bar and hinge simulation. It is based on a standard bar and hinge model with N4B5 panels and linear elastic rotational springs. This package uses an explicit solver so that it can parallelize its computation. With parallelization, the package can compute one loading step orders of magnitude faster than the MERLIN package (measured using wall clock time). However, the package does require manually softening the material stiffness (from its actual value) and using a much shorter loading step to obtain converging results. OMTO by Kazuko Fuchi and the nonlinear truss package by Andrew Gillman [149,150,233,234] are two other bar and hinge-type implementation specially designed for topological optimization applications. The underlying folding simulation of this nonlinear truss package is similar to MERLIN but is designed to perform topological optimization of origami systems. Both the MERLIN package [204] and the nonlinear truss package [233,234] can capture localized panel contact and prevent creases from folding more than 180 deg (see Fig. 19(a) and 19(b)). SWOMPS [64] is a MATLAB-based implementation of the bar and hinge simulation. The package uses a generalized N5B8 panel model and allows users to choose between a simple rotational spring crease model and a compliant crease model. swomps can simulate global panel contact (see Fig. 19(c)), can approximate panel thickness, can capture electrothermalmechanically coupled actuation within active origami, and can allow for sequential and arbitrary loading of the origami.

In general, these bar and hinge simulation implementations are suitable for studying the kinematics, capturing the mechanical and nonmechanical properties, simulating the active folding, and performing pattern optimization of origami systems. The simulations have the capability of real-time simulation [195], and can be updated for rapid simulations of origami with multiphysics [64]. However, because these bar and hinge simulations use coarse meshes for the origami systems, these packages are only suitable for capturing global behaviors. Localized nonlinear behaviors

such as panel buckling, kinking, and stress concentrations are beyond the capabilities of these packages.

Finally, a number of commercial software programs and the associated extension packages can also be used to simulate origami systems. Rhino and Grasshopper-based physics-engine Kangaroo [219] can be used to capture origami systems. The Crane package [235] is an extension that implements the Freeform origami algorithm within the Rhino and Grasshopper environment. The Rhino and Grasshopper environment is suitable for parametric design of origami systems and is widely used by designers and architects. When high-accuracy simulations are needed, commercial FE software programs tend to be used. A variety of different FE software programs have been used for simulating the behaviors of origami systems such as ABAQUS [139,172–174,176–179, 182–186], ANSYS [39,180,187], LS-DYNA [175,180,181], and COMSOL [65,228]. These packages also support origami researchers to create user-defined elements. For example, the work by Hu et al. [168] created a small-strain plate model for simulating origami panels with small curvature deformation that are more computationally efficient than using the fine meshed FE models. Using commercial FE software programs can achieve high fidelity solutions and capture localized nonlinear behaviors in origami systems. However, using FE simulations requires longer computation time and an extended model building schedule. In addition, FE simulations can act like "black boxes" in some situations, which make them not suitable for developing fundamental theories of origami structures.

#### 7 Selecting and Developing Appropriate Simulations

In this section, we discuss how to select or develop a simulation technique for capturing the behavior of origami systems. After evaluating the challenges in selecting and developing appropriate techniques, we present a flowchart to help guide the process, along with a number of accompanying case studies.

Appropriate Models: What constitutes an appropriate model for a particular origami system demands a significant element of judgment from the engineer or scientist investigating the problem. A common guiding scientific principle (Occam's Razor) is to use the simplest model that still captures the observed behavior of interest. This model might be called a "minimal model." In many cases, lower fidelity models with a greater number of assumptions provide greater insight into the behavior of origami systems. Consider, for instance, the analysis of rigid-foldable origami systems; these systems can be modeled using high-fidelity FE models, but this approach will not provide an understanding of the mathematical conditions for rigid-foldability that could be obtained from kinematics-based modeling [55]. Moreover, reduced-order bar and hinge models can provide insight into the mechanics of an origami system, not offered by detailed FE models with continuum elements. For example, in the study of bistable origami hypars [146], comparing different bar and hinge meshes

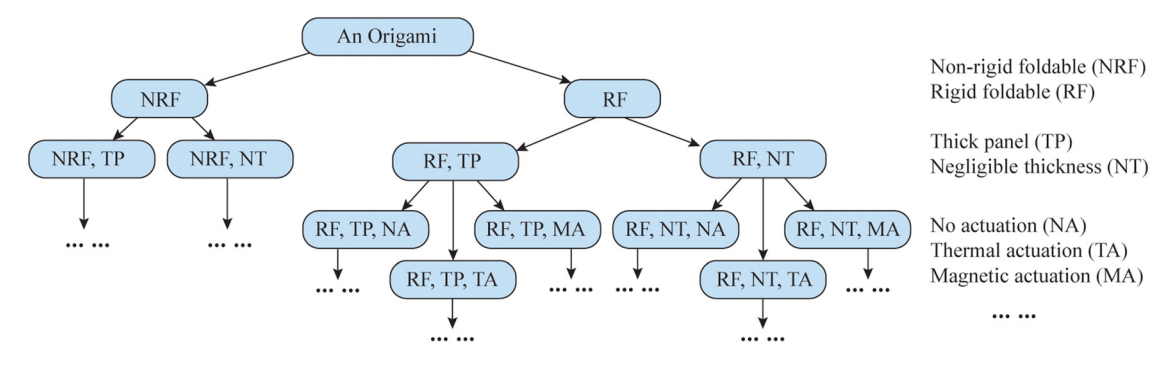


Fig. 21 A universal origami modeling approach is not achievable; instead, there is an exponential growth in tailored models that can capture distinct properties and characteristics for individual origami problems

(i.e., with different panel bending direction) provides insight into which deformations are most significant to the bistability of origami hypars. Similarly, in the analysis of origami tubes [171], the bar and hinge models provide a method to independently change the in-plane, bending, and folding stiffness to gain insight into the dominant contributors. These types of comparative studies are difficult to execute in FE models. Finally, such minimal models can reveal theoretical connections between origami and other disciplines, which helps origami engineers develop new models. For example, the development of thick and rigid origami models has revealed the close connection between origami and linkage mechanisms [108].

From an engineering perspective, an appropriate origami models should also consider the balance between the computation time and the model fidelity. Solving high fidelity models not only requires longer computation time but also requires more sophisticated solution methods. Here, computation time could refer to the number of floating point operations (not affected by the programing language that is used), the wall-clock run time (affected by the programing language), or even the duration of developing and implementing a simulation. An illustrative example where computation time and model simplicity are traded off against fidelity is the analysis of tubular origami structures such as the Kresling pattern; their nonrigid foldable properties require the use of a mechanics-based model. In various works, the behavior of the Kresling pattern is captured using a bar and hinge model [63,156,236] because it captures the panel deformation, is computationally efficient, and rapid to setup for different geometries. However, bar and hinge models cannot capture the buckling of crease lines, which are observed in some physical experiments [196]. Masana and Dagag therefore modified their formulation of the bar and hinge model by introducing additional nodes and springs along the fold lines [196]. These additional nodes and springs allow the creases to buckle so that the model can better capture the global physical behavior. An alternative to capture this local crease buckling in the Kresling pattern is to use FE models as shown in the work by Hwang [237]. Another consideration is the time required to formulate the model and setup the simulation for a specific problem. In this case, human factors can play a large role. A researcher familiar with reduced-order models may choose the bar and hinge approach as in Ref. [196] and a researcher familiar with commercial FE packages may choose the FE models as in Ref. [237]. These cases illustrate that finding a "balanced" model is subjective, and in addition to the features of the different model options, people should also consider their prior knowledge and experience.

Finally, as the community continues to design increasingly sophisticated origami structures for engineering applications, selecting and developing origami models becomes more complex due to the exponentially growing number of origami characteristics that need to be captured; see Fig. 21. This exponential growth makes it challenging to find a minimal model that satisfies the desire for simplicity or a balanced model that trades optimum speed and fidelity.

Flowchart: To help navigate the complexity of selecting and developing origami simulation techniques, we offer a nonexhaustive flowchart, shown in Fig. 22, to aid the selection and development process. The three aspects to consider when selecting and building simulation techniques are: the origami characteristics, objectives of the simulation, and other factors. To select an appropriate simulation for origami, the left flowchart identifies potential simulations that can capture the target characteristics of the origami systems, and the right flowchart helps find a simulation that fits the given objectives. Once a potential simulation technique is identified, other factors such as available facilities and capabilities can be taken into consideration. In developing a new or modified simulation technique, the flowchart can help users select a base simulation technique. The following text discusses the flowchart and presents a number of examples.

Starting with the flowchart for origami characteristics in box 1 of Fig. 22, one of the most fundamental features of an origami system is whether it is rigid-foldable or not. If the origami is rigid-foldable, their folding motions can be captured using kinematic simulations or rigid panel based mechanical simulations (item 1.1). However, if the origami is nonrigid-foldable, simplified mechanical simulations like the bar and hinge simulations [63,145] and the plate theory-based simulations [168,169] or more advanced options like FE simulations are needed (item 1.2). Next, more detailed features of the origami system can be considered. For example, studying rigid-foldable origami with non-negligible compliant creases can be accomplished using the smooth fold simulations [103,104,106] (item 1.1.1), while studying the nonrigidfoldable origami with non-negligible compliant creases can use compliant crease bar and hinge simulations [136], plate theorybased simulations [167], or FE simulations [189] (item 1.2.1).

In addition to the properties of the origami, the objectives of the simulation should also be considered, as shown in box 2 of Fig. 22. Broadly, there are three types of objectives that may be of interest: to study the origami folding motion, to study the change in origami properties, and to achieve pattern design and shape fitting. For the simulation of origami folding motions, the primary factor to consider is its means of actuation; if no actuation mechanisms are considered, conventional kinematic and mechanical origami simulation techniques can be used (item 2.1.1). On the other hand, if multiphysics actuation is intended (item 2.1.2), building new origami simulations may be necessary. For example, Swaminathan et al. [210] introduce a magnetic actuation module into a physics-based origami simulation program. Capturing the property changes in origami is a common objective in origami simulation. For changes in the kinematic and mechanical properties, using existing origami simulations tends to be sufficient (item 2.2.1 to 2.2.3), but analyzing multiphysical properties may require combining different simulation environments, as discussed in Sec. 5. In this case, finding an origami simulation technique that integrates with other multiphysics simulation environments can become crucial (item 2.2.4). Finally, selecting simulations for pattern design and origami shape fitting focuses more on the balance between the computational speed and the model fidelity (item 2.3). In general, kinematics simulations and reduced-order mechanical simulations are preferred for such objectives.

Case Studies: Finally, we present a number of case studies on selecting and developing origami simulations. The first example is to design an origami that fits a desired target surface (item 2.3 in Fig. 22). Research efforts have mainly focused on using rigid-foldable patterns for shape fitting [87,106,121], with potential applications as deployable structures. As indicated in item 1.1 and item 2.3, kinematic simulations are popular for this objective because they are computationally efficient [13,87,106,121,238]. Moreover, some of these kinematic simulations can be extended such that origami structures with thick panels [126] or those with compliant creases [106] can also be designed in a similar fashion (item 1.1.2). Alternatively, reduced-ordered mechanical simulations for origami could be used because they can capture nonrigid foldable origami [149,150] while also remaining computationally efficient (item 1.1).

The second example is the analysis of origami FSS. A number of publications have studied the performance of origami FSS, often using the Miura-ori pattern [38,39,222–225]. Because the Miura-ori tessellation is rigid-foldable, a simulation technique from item 1.1 on Fig. 22 can be employed to capture the geometry. However, capturing the electromagnetic properties of the origami FSS requires more sophisticated electromagnetic simulations and is thus performed using separate simulation packages (item 2.2.4). In this case, it is important to build an origami simulation that can output and transfer the origami geometry to the separate simulation package smoothly.

Finally, consider origami for use as an energy absorption system or as a metamaterial with graded stiffness. The objective of such simulations is to find the mechanical properties of the origami (item 2.2.2 or item 2.2.3 in Fig. 22). Usually, the origami structure will experience large panel deformations with potential panel contact, as listed in item 1.2.3. Here, FE simulations can be the preferred choice because they are capable of capturing nonlinear and plastic deformations [139,186]. However, if the origami is rigid-foldable and does not experience large panel deformations, a reduced-order mechanical simulation may also be suitable [4,158,239].

#### **8** Future Challenges and Conclusions

Despite the significant advances in the field of origami simulations, there remains a range of open challenges. Here, we offer our view on key themes within the future challenges: simulation validation, enhancement of simulation capabilities, and integration with design.

**Simulation Validation:** A large number of different simulation techniques have been proposed for capturing the behavior of origami-inspired structures. What are the limits of these simulations? How accurate are these simulations when applied to different origami patterns, across different scales and manufactured from different materials? These are open questions that have not been systematically addressed in existing research. To resolve the problem, we propose the development of a high-quality openaccess library of experimental benchmarks of origami. This approach is inspired by experimental benchmark libraries created for other engineering problems (e.g., radar cross section [240]).

What patterns should be chosen for these high quality experiments? At the very least, the selection should include both rigid foldable patterns (such as the Miura-ori) and nonrigid foldable patterns (such as the Kresling pattern). However, as demonstrated by Pinson et al. [241], the strain energy from origami folding can span orders of magnitude depending on how well the pattern complies with the rigid-foldability conditions; this makes it challenging to select representative patterns that sufficiently capture this energy landscape. In addition, the physical length scale of origami needs to be considered. For example, origami systems at meter and millimeter scale show different responses, because gravity has a greater impact at larger scales. Moreover, what materials should the library contain? The use of paper would seem to be a straightforward answer because of its ubiquitous use in origami prototyping. However, as pointed out by Grey et al. [242], paper is not suitable for validation because of its nonlinear and pseudoplastic behavior. Thus, future benchmarks should consider multiple materials with different elasto-plastic behaviors. Finally, these benchmark experiments should also reflect information on the variability in material properties and dimensions because origami structures can be significantly affected by even small imperfections [147].

**Enhancement of Simulation Capabilities:** Future research needs to enhance the capabilities of current simulation techniques and packages. These enhancements include but are not limited to supporting more elaborate material models, developing advanced multiscale simulations, building multiphysics interaction models,

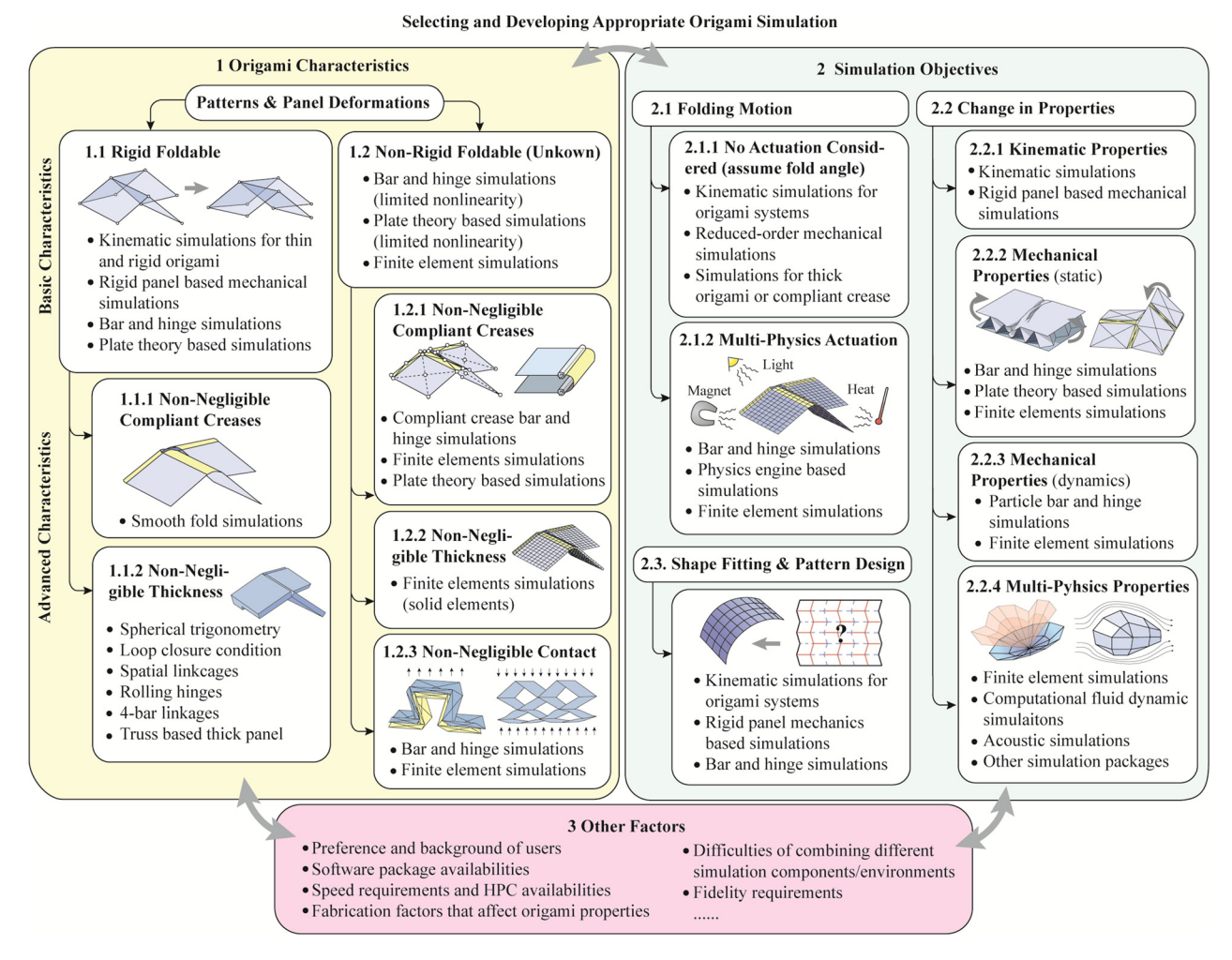


Fig. 22 Considerations for selecting and developing simulation techniques for origami systems

and capturing interaction between origami modules. For instance, current reduced-order origami simulation capabilities have been mostly limited to linear-elastic material models, whereas materials used for origami prototyping and applications are generally nonlinear elasto-plastic [242] and can be further affected by the ambient environment such as temperature and humidity (especially for active folding).

Simulating the global response of origami systems requires accurately capturing local details such as the properties at creases and small manufacturing imperfections [147]. In order to develop origami-inspired systems with increased numbers of unit cells, as might be needed for shape-adaptive surfaces, multiscale simulation techniques should be developed. High-fidelity simulations of local features and unit cell geometry would feed into larger-scale, reduced-order simulations of the behavior of origami systems. Further, in order to better capture the coupling between actuation, response to external stimuli, origami folding, and the nonmechanical properties of origami devices, more comprehensive multiphysics simulations must be developed. Another less visited topic in the simulation of origami is the interaction between origami modules. Many origami-inspired metamaterials are constructed by integrating repeating origami unit cells [7]. These unit cells are often fabricated individually and then assembled to form an origami metamaterial. The interaction between individual origami modules can affect the bulk behavior of the metamaterial, and developing reliable simulations to capture such interactions is also an important task for the future.

Integration of Simulation and Design: Finally, the effective integration of origami simulation with different origami design methodologies remains an open challenge. Currently, many origami simulation techniques and tools are developed without considering how these tools can be systematically integrated into origami design methodologies. A unified workflow, data format, and parameterization of the origami design space would be important for connecting simulation to design. A standardized data format can help origami researchers to develop computational tools more efficiently and the FOLD format [229] demonstrates a first attempt to accomplish this goal. However, further developments are needed to include additional origami properties related to active folding, mechanical behavior, and nonmechanical performance. In addition, improving the accessibility of the simulation package is also important. Many new users of origami simulation software programs may not have prior background in computational mechanics or even general programming. Therefore, future origami simulation packages will need to enhance their accessibility to researchers from noncomputational disciplines and the general public. For example, the Crane package [235] for Rhino/ Grasshopper demonstrates one successful attempt to bring origami design and simulation techniques [91] to the architecture and design community.

In conclusion, in this work we reviewed the state-of-the-art in origami simulations, and broadly categorized origami simulation techniques into kinematics-based, mechanics-based, and multiphysics simulations. We analyzed the underlying origami models and solution methods, discussed the theoretical background of these techniques, evaluated the advantages and disadvantages of different simulations, and demonstrated the connection between origami simulations and other engineering disciplines. Based on the overview of available simulations techniques, we discussed why developing origami simulations is challenging and how to select and develop appropriate origami simulation techniques for specific applications. Finally, we identified promising directions of future research, focusing on simulation validation, enhanced simulation capabilities, and improved integration of simulation and design. Origami simulation is a rapidly evolving field of research and we believe that future developments will yield faster, more robust, and easier-to-use simulation techniques and packages for researchers and designers from different disciplines.

#### Acknowledgment

This work was partially funded by the National Science Foundation (NSF) through Grant Nos. 2054148 and 1943723. The paper reflects the views and position of the authors, and not necessarily those of the funding entity. The authors acknowledge the helpful discussions with Robert Lang and Yutong Xia. The authors also acknowledge the helpful comments and suggestions from the reviewers.

#### **Funding Data**

• Division of Civil, Mechanical and Manufacturing Innovation (Grant Nos. 2054148 and 1943723; Funder ID: 10.13039/ 100000147).

#### References

- [1] Wootton, R. J., 1981, "Support and Deformability in Insect Wings," J. Zool., 193(4), pp. 447-468.
- [2] Dobson, C. M., 2003, "Protein Folding and Misfolding," Nature, 426(6968),
- [3] Fang, H., Li, S., and Wang, K., 2016, "Self-Locking Degree-4 Vertex Origami Structures," Proc. R. Soc. A, 472(2195), p. 20160682
- [4] Fang, H., Chu, S.-C. A., Xia, Y., and Wang, K.-W., 2018, "Programmable Self-Locking Origami Mechanical Metamaterials," Adv. Mater., 30(15), p.
- [5] Schenk, M., and Guest, S. D., 2013, "Geometry of Miura-Folded Metamaterials," Proc. Natl. Acad. Sci., 110(9), pp. 3276-3281.
- [6] Wang, H., Zhao, D., Jin, Y., Wang, M., Mukhopadhyay, T., and You, Z., 2020, "Modulation of Multi-Directional Auxeticity in Hybrid Origami Metamaterials," Appl. Mater. Today, 20, p. 100715.
- [7] Overvelde, J. T., de Jong, T. A., Shevchenko, Y., Becerra, S. A., Whitesides, G. M., Weaver, J. C., Hoberman, C., and Bertoldi, K., 2016, "A Three-Dimensional Actuated Origami-Inspired Transformable Metamaterial With Multiple Degrees of Freedom," Nat. Commun., 7(1), p. 10929.
- [8] Cheung, K. C., Tachi, T., Calisch, S., and Miura, K., 2014, "Origami Interleaved Tube Cellular Materials," Smart Mater. Struct., 23(9), p. 094012.
  [9] Boatti, E., Vasios, N., and Bertoldi, K., 2017, "Origami Metamaterials for
- Tunable Thermal Expansion," Adv. Mater., 29(26), p. 1700360.
- [10] Lv, C., Krishnaraju, D., Konjevod, G., Yu, H., and Jiang, H., 2015, "Origami Based Mechanical Metamaterials," Sci. Rep., 4(1), p. 5979.
  [11] An, B., Benbernou, N., Demain, E. D., and Rus, D., 2011, "Planning to Fold
- Multiple Objects From a Single Self-Folding Sheet," Robotica, 29(1), pp. 87-102.
- [12] An, B., and Rus, D., 2014, "Designing and Programming Self-Folding Sheets," Rob. Auton. Syst., 62(7), pp. 976–1001.
- [13] An, B., Miyashita, S., Ong, A., Tolley, M. T., Demaine, M. L., Demaine, E. D., Wood, R. J., and Rus, D., 2018, "An End-to-End Approach to Self-Folding Origami Structures," IEEE Trans. Rob., 34(6), pp. 1409-1424.
- [14] Felton, S., Tolley, M., Demaine, E., Rus, D., and Wood, R., 2014, "A Method for Building Self-Folding Machines," Science, 345(6197), pp. 644-646.
- [15] Li, S., Vogt, D. M., Rus, D., and Wood, R. J., 2017, "Fluid-Driven Origami-Inspired Artificial Muscles," Proc. Natl. Acad. Sci., 114(50), pp. 13132-13137
- [16] Onal, C. D., Tolley, M. T., Wood, R. J., and Rus, D., 2015, "Origami-Inspired Printed Robots," IEEE/ASME Trans. Mechatronics, 20(5), pp. 2214-2221
- [17] Miyashita, S., Guitron, S., Ludersdorfer, M., Sung, C. R., and Rus, D., 2015, "An Untethered Miniature Origami Robot That Self-Folds, Walks, Swims, and Degrades," IEEE International Conference on Robotics and Automation (ICRA), Seattle, WA, May 26–30, pp. 1490–1496.
- [18] Hawkes, E., An, B., Benbernou, N. M., Tanaka, H., Kim, S., Demaine, E. D., Rus, D., and Wood, R. J., 2010, "Programmable Matter by Folding," Proc. Natl. Acad. Sci., 107(28), pp. 12441–12445.
- [19] Na, J.-H., Evans, A. A., Bae, J., Chiappelli, M. C., Santangelo, C. D., Lang, R. J., Hull, T. C., and Hayward, R. C., 2015, "Programming Reversibly Self-Folding Origami With Micropatterned Photo-Crosslinkable Polymer Trilayers," Adv. Mater., 27(1), pp. 79–85.
- [20] Kang, J.-H., Kim, H., Santangelo, C. D., and Hayward, R. C., 2019, "Enabling Robust Self-Folding Origami by Pre-Biasing Buckling Direction," Adv. Mater., **31**(39), p. 0193006.
- [21] Zhu, Y., Mayur, B., Oldham, K. R., and Filipov, E. T., 2020, "Elastically and Plastically Foldable Electro-Thermal Micro-Origami for Controllable and Rapid Shape Morphing," Adv. Funct. Mater., 30(40), p. 2003741.
- [22] Liu, Q., Wang, W., Reynolds, M. F., Cao, M. C., Miskin, M. Z., Arias, T. A., Muller, D. A., McEuen, P. L., and Cohen, I., 2021, "Micrometer-Sized Electrically Programmable Shape-Memory Actuators for Low-Power Microrobotics," Sci. Rob., 6(52), p. eabe6663.
- [23] Breger, J. C., Yoon, C., Xiao, R., Kwag, H. R., Wang, M. O., Fisher, J. P., Nguyen, T. D., and Gracias, D. H., 2015, "Self-Folding Thermo-Magnetically Responsive Soft Microgrippers," ACS Appl. Mater. Interfaces, 7(5), pp. 3398-3405.
- [24] Yoon, C., Xiao, R., Park, J., Cha, J., Nguyen, T. D., and Gracias, D. H., 2014, "Functional Stimuli Responsive Hydrogel Devices by Self-Folding," Smart Mater. Struct., 23(9), p. 094008.

- [25] Bassik, N., Stern, G. M., and Gracias, D. H., 2009, "Microassembly Based on Hands Free Origami With Bidirectional Curvature," Appl. Phys. Lett., 95(9), o. 091901.
- [26] Leong, T. G., Randall, C. L., Benson, B. R., Bassik, N., Stern, G. M., and Gracias, D. H., 2009, "Tetherless Thermaobiochemically Actuated Microgrippers," Proc. Natl. Acad. Sci., 106(3), pp. 703–708.
- [27] Kuribayashi, K., Tsuchiya, K., You, Z., Tomus, D., Umemoto, M., Ito, T., and Sasaki, M., 2006, "Self-Deployable *Origami* Stent Grafts as a Biomedical Application of Ni-Rich TiNi Shape Memory Alloy Foil," Mater. Sci. Eng.: A,
- **419**(1–2), pp. 131–137. [28] Filipov, E. T., Tachi, T., and Paulino, G. H., 2015, "Origami Tubes Assembled Into Stiff yet Reconfigurable Structures and Metamaterials," Proc. Natl. Acad. Sci., 40(112), pp. 12321–12326.
- [29] Melancon, D., Gorissen, B., Garcia-Mora, C. J., Hoberman, C., and Bertoldi, K., 2021, "Multistable Inflatable Origami Structures at the Metre Scale," Nature, **592**(7855), pp. 545–550.
- [30] Liu, X., Gattas, J. M., and Chen, Y., 2016, "One-DOF Superimposed Rigid Origami With Multiple States," Sci. Rep., 6(1), p. 36883.
- [31] Babilio, E., Miranda, R., and Fraternali, F., 2019, "On the Kinematics and Actuation of Dynamic Sunscreens With Tensegrity Architecture," Front. Mater., 6, p. 7.
- Lang, R. J., Magleby, S., and Howell, L., 2016, "Single Degree-of-Freedom Rigidly Foldable Cut Origami Flashers," ASME J. Mech. Rob., 8(3), p.
- [33] Kaddour, A.-S., Velez, C. A., Hamza, M., Brown, N., Ynchausti, C., Magleby, S. P., Howell, L., and Georgakopoulos, S. V., 2020, "A Foldable and Reconfigurable Monolithic Reflect Array for Space Application," IEEE Access, 8, op. 219355-219366.
- [34] Wilson, L., Pellegrino, S., and Danner, R., 2013, "Origami Sunshield Concepts for Space Telescopes," Structures, Structural Dynamics, and Materials and Co-Located Conferences, Boston, MA, April 8-11, p. 12.
- [35] Seymour, K., Burrow, D., Avila, A., Bateman, T., Morgan, D. C., Magleby, S. P., and Howell, L. L., 2018, "Origami Based Deployable Ballistic Barrier,"
- Origami 7, Tarquin, St Albans, UK, pp. 763–778.

  [36] Tolman, K., Crampton, E., Stucki, C., Maynes, D., and Howell, L. L., 2018, "Design of an Origami-Inspired Deployable Aerodynamic Locomotive Fairing," *Origami 7*, Tarquin, St Albans, UK, pp. 669–684.
  [37] DeFigueiredo, B. P., Pehrson, N. A., Tolman, K. A., Crampton, E., Magleby,
- S. P., and Howell, L. L., 2019, "Origami-Based Design of Conceal-and-Reveal Systems," ASME J. Mech. Rob., 11(2), p. 020904.
- [38] Nauroze, S. A., and Tentzeris, M. M., 2019, "A Thermally Actuated Fully Inkjet-Printed Origami Inspired Multilayer Frequency Selective Surface With Continuous-Range Tunability Using Polyester-Based Substrates," IEEE Trans. Microwave Theory Tech., 67(12), pp. 4944-4954.
- [39] Nauroze, S. A., Novelino, L. S., Tentzeris, M. M., and Paulino, G. H., 2018, 'Continuous-Range Tunable Multilayer Frequency-Selective Surfaces Using Origami and Inkjet Printing," Proc. Natl. Acad. Sci., 115(52), pp. 13210-13215
- [40] Babaee, S., Overvelde, J. T. B., Chen, E. R., Tournat, V., and Bertoldi, K., 2016, "Reconfigurable Origami-Inspired Acoustic Wave Guides," Sci. Adv., 2(11), p. e1601019.
- [41] Balkcom, D. J., Demaine, E. D., Demaine, M. L., Ochsendorf, J. A., and You, Z., 2009, "Folding Paper Shopping Bags," Origami 4, A K Peters, Natick, MA, pp. 315-334.
- [42] Liu, C., and Felton, S. M., 2018, "Transformation Dynamics in Origami," Phys. Rev. Lett., **121**(25), p. 254101.
- [43] Li, S., and Wang, K. W., 2015, "Fluidic Origami: A Plant-Inspired Adaptive Structure With Shape Morphing and Stiffness Tuning," Smart Mater. Struct., 24(10), p. 105031.
- [44] Rogers, J., Huang, Y., Schmidt, O. G., and Gracias, D. H., 2016, "Origami MEMS and NEMS," MRS Bull., 41(2), pp. 123–129.
  [45] Li, S., Fang, H., Sadeghi, S., Bhovad, P., and Wang, K.-W., 2019,
- 'Architected Origami Materials: How Folding Creates Sophisticated Mechanical Properties," Adv. Mater., 31(5), p. 1805282.
- [46] Quinones, V. A. B., Zhu, H., Solovev, A. A., Mei, Y., and Gracias, D. H., 2018, "Origami Biosystems: 3D Assembly Methods for Biomedical Applications," Adv. Biosyst., 2(12), p. 1800230.
- [47] Rus, D., and Tolley, M. T., 2018, "Design, Fabrication and Control of Origami Robots," Nat. Rev. Mater., 3(6), pp. 101-112.
- [48] Meloni, M., Cai, J., Zhang, Q., Lee, D. S.-H., Li, M., Ma, R., Parashkevov, T. E., and Feng, J., 2021, "Engineering Origami: A Comprehensive Review of Recent Applications, Design Methods, and Tools," Adv. Sci., 8(13), p.
- [49] Lebee, A., 2015, "From Folds to Structures, A Review," Int. J. Space Struct., 30(2), pp. 55-74
- [50] Lang, R., 2018, Twists, Tilings, and Tessellations: Mathematical Methods for Geometric Origami, CRC Press, Boca Raton, FL.
- [51] Huffman, D. A., 1976, "Curvature and Creases: A Primer on Paper," IEEE Trans. Comput., C-25(10), pp. 1010–1019.
- [52] Resch, R., and Christiansen, H. N., 1970, "Kinematic Folded Plate System," Proceedings of IASS Symposium on Folded Plates and Prismatic Structures, Vienna, Austria, Sept./Oct.
- [53] Kawasaki, T., and Yoshida, M., 1988, "Crystallographic Flat Origamis," Mem. Fac. Sci., Kyushu Univ., 42(2), pp. 153–157.
- Kawasaki, T., 1989, "On the Relation Between Mountain-Creases and Valley-Creases of a Flat Origami," Proceedings of First International Meeting Origami of Science and Technology, Universita di Padova, Italy, Dec. 6-7, pp. 153-157.

- [55] Belcastro, S.-M., and Hull, T. C., 2002, "Modelling the Folding of Paper Into Three Dimensions Using Affine Transformations," Linear Algebra Appl., 348(1-3), pp. 273-282.
- [56] Tachi, T., 2009, "Simulation of Rigid Origami," Origami 4, CRC Press/Caltech, Pasadena, CA, pp. 175-187.
- [57] Mitani, J., 2008, "The Folded Shape Restoration and the Rendering Method of Origami From the Crease Pattern," 13th International Conference on Geometry and Graphics, Dresden, Germany, Aug. 4–10, p. 7. [58] Guest, S. D., and Pellegrino, S., 1994, "The Folding of Triangulated Cylinders,
- Part II: The Folding Process," ASME J. Appl. Mech., 61(4), pp. 778-783.
- [59] Guest, S. D., and Pellegrino, S., 1996, "The Folding of Triangulated Cylinders, Part III: Experiments," ASME J. Appl. Mech., 63(1), pp. 77-83.
- [60] Yang, N., and Silverberg, J. L., 2017, "Decoupling Local Mechanics From Large-Scale Structure in Modular Metamaterials," Proc. Natl. Acad. Sci., 114(14), pp. 3590-3595.
- [61] Schenk, M., and Guest, S. D., 2010, "Origami Folding: A Structural Engineering Approach," Origami 5, CRC Press, Singapore, pp. 293-305.
- [62] Wei, Z. Y., Guo, Z. V., Dudte, L., Liang, H. Y., and Mahadevan, L., 2013, 'Geometric Mechanics of Periodic Pleated Origami," Phys. Rev. Lett., 110(21), p. 215501.
- [63] Liu, K., and Paulino, G., 2017, "Nonlinear Mechanics of Non-Rigid Origami: An Efficient Computational Approach," Proc. R. Soc. A, 473(2206), p. 20170348.
- [64] Zhu, Y., and Filipov, E. T., 2021, "Rapid Multi-Physics Simulation for Electro-Thermal Origami Systems," Int. J. Mech. Sci., 202-203, p. 106537.
- [65] Hathcock, M., Popa, B.-I., and Wang, K. W., 2021, "Origami Inspired Phononic Structure With Metamaterial Inclusions for Tunable Angular Wave Steering," J. Appl. Phys., 129(14), p. 145103.
- [66] Dias, M. A., Dudte, L. H., Mahadevan, L., and Santangelo, C. D., 2012, "Geometric Mechanics of Curved Crease Origami," Phys. Rev. Lett., 109(11), . 114301
- [67] Butler, J., Pehrson, N., and Magleby, S., 2020, "Folding of Thick Origami Through Regionally Sandwiched Compliant Sheets," ASME J. Mech. Rob., 12(1), p. 011019.
- [68] Mitani, J., 2012, "ORIPA," University of Tsukuba, Tsukuba, Japan, accessed Dec. 2021, https://mitani.cs.tsukuba.ac.jp/oripa/
- [69] Lang, R. J., and Howell, L. L., 2018, "Rigidly Foldable Quadrilateral Meshes From Angle Arrays," ASME J. Mech. Rob., 10(2), p. 021004.
- [70] Evans, A. A., Silverberg, J. L., and Santangelo, C. D., 2015, "Lattice Mechanics of Origami Tessellations," Phys. Rev. E, 92(1), p. 013205.
- [71] Evans, T. A., Lang, R. J., Magleby, S. P., and Howell, L. L., 2015, "Rigidly Foldable Origami Gadgets and Tessellations," R. Soc. Open Sci., 2(9), p.
- [72] Evans, T. A., Lang, R. J., and Magleby, S. P., 2015, "Rigidly Foldable Origami Twists," Origami 6, American Mathematical Society, Providence, RI, pp. 119-130.
- [73] Tachi, T., 2009, "Generalization of Rigid Foldable Quadrilateral Mesh Origami," J. Int. Assoc. Shell Spatial Struct., 50, pp. 173-179.
- [74] Hull, T., 2013, Project Origami, CRC Press, Boca Raton, FL.
- [75] Zimmermann, L., Shea, K., and Stankovic, T., 2020, "Conditions for Rigid and Flat Foldability of Degree-n Vertices in Origami," ASME J. Mech. Rob., 12(1), p. 011020.
- [76] Waitukaitis, S., Menaut, R., Chen, B. G., and van Hecke, M., 2015, "Origami Multistability: From Single Vertices to Metasheets," Phys. Rev. Lett., 114, p. 055503
- [77] Kamrava, S., Mousanezhad, D., Ebrahimi, H., Ghosh, R., and Vaziri, A., 2017, "Origami-Based Cellular Metamaterial With Auxetic, Bistable and Self-
- Locking Properties," Sci. Rep., 7(1), p. 46046. [78] Kamrava, S., Mousanezhad, D., Felton, S. M., and Vaziri, A., 2018, "Programmable Origami Strings," Adv. Mater. Technol., 3(3), p. 1700276.
- [79] Hanna, B. H., Lund, J. M., Lang, R. J., Magleby, S. P., and Howell, L. L., 2014, "Waterbomb Base: A Symmetric Single-Vertex Bistable Origami Mechanism," Smart Mater. Struct., 23(9), p. 094009.
- [80] Silverberg, J. L., Evans, A. A., McLeod, L., Hayward, R. C., Hull, T., Santangelo, C. D., and Cohen, I., 2014, "Using Origami Design Principles to Fold Reprogrammable Mechanical Metamaterials," Science, 345(6197), pp. 647-650.
- [81] Yasuda, H., Yein, T., Tachi, T., Miura, K., and Taya, M., 2013, "Folding Behaviour of Tachi-Miura Polyhedron Bellows," Proc. R. Soc. A, 469(2159),
- [82] Yasuda, H., and Yang, J., 2015, "Reentrant Origami-Based Metamaterials With Negative Poisson's Ratio and Bistability," Phys. Rev. Lett., 114(18), p.
- [83] Wu, W., and You, Z., 2011, "A Solution for Folding Rigid Tall Shopping Bags," Proc. R. Soc. A, 467(2133), pp. 2561-2574.
- [84] Tachi, T., 2010, "Geometric Considerations for the Design of Rigid Origami Structures," Proceedings of the International Association for Shell and Spatial Structures (IASS) Symposium, Shanghai, China, Nov. 8-12, International Association for Shell and Spatial Structures, p. 12.
- [85] Hu, Y., and Liang, H., 2020, "Folding Simulation of Rigid Origami With
- Lagrange Multiplier Method," Int. J. Solids Struct., 202, pp. 552–561.
  [86] Xi, Z., and Lien, J.-M., 2015, "Folding and Unfolding Origami Tessellation by Reusing Folding Path," IEEE International Conference on Robotics and Automation (ICRA), Seattle, WA, May 26-30, pp. 4155-4160.
- [87] Feng, F., Dang, X., James, R. D., and Plucinsky, P., 2020, "The Designs and Deformations of Rigidly and Flat-Foldable Quadrilateral Mesh Origami," J. Mech. Phys. Solids, 142, p. 104018.

- [88] Peng, R., Ma, J., and Chen, Y., 2017, "Rigid Foldability of Triangle Twist Origami Pattern and Its Derived 6R Linkage," ASME Paper No. DETC2017-68063.
- [89] Bowen, L. A., Baxter, W. L., Magleby, S. P., and Howell, L. L., 2014, "A Position Analysis of Coupled Spherical Mechanisms Found in Action
- Origami," Mech. Mach. Theory, 77, pp. 13–24.
  Wei, G., and Dai, J. S., 2014, "Origami-Inspired Integrated Planar-Spherical Overconstrained Mechanisms," ASME J. Mech. Des., 136(5), p. 051003.
- [91] Tachi, T., 2010, "Freeform Variations of Origami," J. Geometry Graph., 14(2), pp. 203-215.
- [92] Demaine, E. D., and Tachi, T., 2017, "Origamizer: A Practical Algorithm for Folding Any Polyhedron," 33rd International Symposium on Computational Geometry (SoCG 2017), B. Aronov, and M. J. Katz, eds., Schloss Dagstuhl-Leibniz-Zentrum Fuer Informatik, Dagstuhl Oublishing, Germany, pp. 34:1-34:16.
- [93] Tachi, T., 2010, "Origamizing Polyhedral Surfaces," IEEE Trans. Visualization Comput. Graph., 16(2), pp. 298-311.
- [94] Tachi, T., 2013, "Designing Freeform Origami Tessellations by Generalizing Resch's Patterns," ASME J. Mech. Des., 135(11), p. 111006.
- [95] Feng, F., Plucinsky, P., and James, R. D., 2020, "Helical Miura Origami," Phys. Rev. E, 101(3), p. 033002.
- [96] Silverberg, J. L., Na, J.-H., Evans, A. A., Liu, B., Hull, T. C., Santangelo, C. D., Lang, R. J., Hayward, R. C., and Cohen, I., 2015, "Origami Structures With a Critical Transition to Bistability Arising From Hidden Degrees of Freedom," Nat. Mater., 14(4), pp. 389-393.
- [97] Tachi, T., 2020, "Freeform Origami," The University of Tokyo, Tokyo, Japan, accessed Dec. 2021, https://tsg.ne.jp/TT/software/index.html
  [98] Wu, W., and You, Z., 2010, "Modelling Rigid Origami With Quaternions and
- Dual Quaternions," Proc. R. Soc. A, 466(2119), pp. 2155–2174.
- [99] Broyles, Z., Talbot, S., Johnson, J., Halverson, D. M., and Howell, L. L., 2020, "Unpacking the Mathematics of Modeling Origami Folding Transformations With Quaternions," Proceedings for the USCTOMM Symposium on Mechanical Systems and Robotics, Vol. 83, Springer, Cham, pp. 225–241.

  [100] Cai, J., Zhang, Y., Xu, Y., Zhou, Y., and Feng, J., 2016, "The Foldability of
- Cylindrical Foldable Structures Based on Rigid Origami," ASME J. Mech. Des., 138(3), p. 031401.
- [101] Cai, J., Liu, Y., Ma, R., Feng, J., and Zhou, Y., 2017, "Nonrigidly Foldability Analysis of Kresling Cylindrical Origami," ASME J. Mech. Rob., 9, p. 041018.
- [102] Chen, Y., Sareh, P., Yan, j., Fallah, A. S., and Feng, J., 2019, "An Integrated Geometric-Graph-Theoretical Approach to Representing Origami Structures and Their Corresponding Truss Framework," ASME J. Mech. Des., 141(9), p.
- [103] Hernandez, E. P., Hartl, D. J., and Lagoudas, D. C., 2016, "Kinematics of Origami Structures With Smooth Folds," ASME J. Mech. Rob., 8(6), p.
- [104] Hernandez, E. P., Hartl, D. J., Akleman, E., and Lagoudas, D. C., 2016, "Modeling and Analysis of Origami Structures With Smooth Folds," Comput.-Aided Des., 78, pp. 93–106.
- [105] Hernandez, E. P., Hartl, D. J., and Lagoudas, D. C., 2017, "Analysis and Design of an Active Self-Folding Antenna," ASME Paper No. DETC2017-67855.
- [106] Hernandez, E. A. P., Hartl, D. J., and Lagoudas, D. C., 2017, "Design and Simulation of Origami Structures With Smooth Folds," Proc. R. Soc. A, 473(2200), p. 20160716.
- [107] Hur, D. Y., Hernandez, E. P., Galvan, E., Hartl, D., and Malak, R., 2017, "Design Optimization of Folding Solar Powered Autonomous Underwater Vehicles Using Origami Architecture," ASME Paper No. DETC2017-67848.
- [108] Chen, Y., Peng, R., and You, Z., 2015, "Origami of Thick Panels," Science, 349(6246), pp. 396-400.
- [109] Chen, Y., and You, Z., 2012, "Spatial Overconstrained Linkages—The Lost Jade," Explorations in the History of Machines and Mechanisms, Vol. 15, Springer, Dordrecht, The Netherlands, pp. 535–550.
- [110] Lang, R. J., Nelson, T., Magleby, S., and Howell, L., 2017, "Thick Rigidly Foldable Origami Mechanisms Based on Synchronized Offset Rolling Contact Elements," ASME J. Mech. Rob., 9(2), p. 021013.
- [111] Cai, J., Qian, Z., Jiang, C., Feng, J., and Xu, Y., 2016, "Kinematic Analysis of Foldable Plate Structures With Rolling Joints," ASME J. Mech. Rob., 8(6), p.
- [112] Lang, R. J., Brown, N., Ignaut, B., Magleby, S., and Howell, L., 2020, "Rigidly Foldable Thick Origami Using Designed-Offset Linkages," ASME J. Mech. Rob., 12(2), p. 021106.
- [113] Demaine, E. D., and O'Rourke, J., 2007, Geometric Folding Algorithm, Cambridge University Press, Cambridge, UK.
- [114] Filipov, E. T., Paulino, G. H., and Tachi, T., 2019, "Deployable Sandwich Surfaces With High Out-of-Plane Stiffness," J. Struct. Eng., 145(2), p. 04018244.
- [115] Justin, J., 1989, "Mathematical Aspects of Paper Folding," Proceedings of the First International Meeting of Origami Science and Technology, Universita di Padova, Italy, Dec. 6-9, pp. 263-277.
- [116] Kasahara, K., and Takahama, T., 1987, Origami for the Connoisseur, Japan Publications, JP.
- [117] Bern, M., and Hayes, B., 1996, "The Complexity of Flat Origami," Annual ACM-SIAM Symposium on Discrete Algorithms (SODA), Atlanta, GA, Jan. 28-30, pp. 175-183.
- [118] Hull, T., 1994, "On the Mathematics of Flat Origamis," Congr. Numer., 100, pp. 215-224.

- [119] Mitani, J., and Igarashi, T., 2011, "Interactive Design of Planar Curved Folding by Reflection," Pacific Graphics Short Papers, B.-Y. Chen, J. Kautz, T.-Y. Lee, and M. C. Lin, eds., The Eurographics Association.
- [120] Chen, Y., Feng, H., Ma, J., Peng, R., and You, Z., 2016, "Symmetric Water-bomb Origami," Proc. R. Soc. A, 472(2190), p. 20150846.
- [121] Zhao, Y., Endo, Y., Kanamori, Y., and Mitani, J., 2018, "Approximating 3D Surfaces Using Generalized Waterbomb Tessellations," J. Comput. Des. Eng., 5(4), pp. 442-448.
- [122] Wang, Z. J., Zhou, H., Khaliulin, V. I., and Shabalov, A. V., 2018, "Six-Ray Folded Configurations as the Geometric Basis of Thin-Walled Element in Engineering Structures," Thin-Walled Struct., 130, pp. 435–448.
- [123] Velvaluri, P., Soor, A., Plucinsky, P., de Miranda, R. L., James, R. D., and Quandt, E., 2021, "Origami-Inspired Thin-Film Shape Memory Alloy Devices," Sci. Rep., 11(1), p. 10988.
- [124] Saito, K., Tsukahara, A., and Okabe, Y., 2016, "Designing of Self-Deploying Origami Structures Using Geometrically Misaligned Crease Patterns," Proc. R. Soc. A, 472(2185), p. 20150235.
- [125] Lang, R. J., Tolman, K. A., Crampton, E. B., Magleby, S. P., and Howell, L. L., 2018, "A Review of Thickness Accommodation Techniques in Origami-Inspired Engineering," Appl. Mech. Rev., 70(1), p. 010805.
- [126] Tachi, T., 2011, "Rigid-Foldable Thick Origami," Origami 5, CRC Press, Boca Raton, FL, pp. 253-264.
- [127] Edmondson, B. J., Lang, R. J., Magleby, S. P., and Howell, L. L., 2014, "An Offset Panel Technique for Thick Rigidly Foldable Origami," ASME Paper No. DETC2014-35606.
- [128] Edmondson, B. J., Lang, R. J., Morgan, M. R., Magleby, S. P., and Howell, L. L., 2016, "Thick Rigidly Foldable Structures Realized by an Offset Panel Technique," Origami 6, Vol. 1, American Mathematical Society, Providence, RI, pp. 149–161.
- [129] Ku, J. S., and Demaine, E. D., 2016, "Folding Flat Crease Patterns With Thick
- Materials," ASME J. Mech. Rob., **8**(3), p. 031003. [130] Hoberman, C., 1991, "Reversibly Expandable Structure," U.S. Patent No. 4.981.732.
- [131] Hoberman, C., 1988, "Reversibly Expandable Three Dimensional Structure," U.S. Patent No. 4,780,344.
- [132] Delimont, I. L., Magleby, S. P., and Howell, L. L., 2015, "Evaluating Compliant Hinge Geometries for Origami-Inspired Mechanisms," ASME J. Mech. Rob., 7(1), p. 011009.
- [133] Liu, Y., Boyles, J. K., Genzer, J., and Dickey, M. D., 2011, "Self-Folding of Polymer Sheets Using Local Light Absorption," Soft Mater., 8(6), pp. 513-0273.
- [134] Mao, Y., Yu, K., Isakov, M. S., Wu, J., Dunn, M. L., and Qi, H. J., 2015, 'Sequential Self-Folding Structures by 3D Printed Shape Memory Polymers," Sci. Rep., 5(1), p. 13616.
- [135] Zhu, Y., and Filipov, E., 2019, "Simulating Compliant Crease Origami With a Bar and Hinge Model," ASME Paper No. DETC2019-97119.
- [136] Zhu, Y., and Filipov, E. T., 2020, "A Bar and Hinge Model for Simulating Bistability in Origami Structures With Compliant Creases," ASME J. Mech. Rob., 12(2), p. 021110.
- [137] Chopra, A. K., 2014, Dynamics of Structures, 4th ed., Pearson, London, UK.
- [138] Clough, R. W., and Penzien, J., 1975, Dynamics of Structures, 2nd ed., McGraw-Hill College, New York.
- [139] Ma, J., Song, J., and Chen, Y., 2018, "An Origami-Inspired Structure With Graded Stiffness," Int. J. Mech. Sci., 136, pp. 134–142.
- [140] Leon, S. E., Paulino, G. H., Pereira, A., Menezes, I. F. M., and Lages, E. N., 2011, "A Unified Library of Nonlinear Solution Schemes," ASME. Appl. Mech. Rev., 64(4), p. 040803.
- [141] Zhang, T., Kawaguchi, K., and Wu, M., 2018, "A Folding Analysis Method for Origami Based on the Frame With Kinematic Indeterminacy," Int. J. Mech. Sci., **146–147**, pp. 234–248.
- [142] Zhang, T., and Kawaguchi, K., 2021, "Folding Analysis for Thick Origami With Kinematic Frame Models Concerning Gravity," Autom. Constr., 127, p. 103691.
- [143] Hayakawa, K., and Ohsaki, M., 2021, "Form Generation of Rigid Origami for Approximation of a Curved Surface Based on Mechanical Property of Partially Rigid Frames," Int. J. Solids Struct., 216, pp. 182–199.
- [144] Hayakawa, K., and Ohsaki, M., 2019, "Optimization Approach to Form Generation of Rigid-Foldable Origami for Deployable Roof Structure," The World Congress of Structural and Multidisciplinary Optimization, Beijing, China, May 20-24, p. 6.
- [145] Filipov, E. T., Liu, K., Tachi, T., Schenk, M., and Paulino, G. H., 2017, "Bar and Hinge Models for Scalable Analysis of Origami," Int. J. Solids Struct., 124(1), pp. 26-45.
- [146] Filipov, E. T., and Redoutey, M., 2018, "Mechanical Characteristics of the Bistable Origami Hypar," Extreme Mech. Lett., 25, pp. 16-26.
- [147] Liu, K., Novelino, L. S., Gardoni, P., and Paulino, G. H., 2020, "Big Influence of Small Random Imperfections in Origami-Based Metamaterials," Proc. R. Soc. A, 476(2241), p. 20200236.
- [148] Liu, K., Tachi, T., and Paulino, G. H., 2019, "Invariant and Smooth Limit of Discrete Geometry Folded From Bistable Origami Leading to Multistable Metasurfaces," Nat. Commun., 10(1), p. 4238.
- [149] Gillman, A., Fuchi, K., and Buskohl, P. R., 2018, "Truss-Based Nonlinear Mechanical Analysis for Origami Structures Exhibiting Bifurcation and Limit Point Instabilities," Int. J. Solids Struct., 147, pp. 80–93.
- [150] Gillman, A. S., Fuchi, K., and Buskohl, P. R., 2019, "Discovering Sequenced Origami Folding Through Nonlinear Mechanics and Topology Optimization,' ASME J. Mech. Des., 141(4), p. 041401.

- [151] Kaufmann, J., Bhovad, P., and Li, S., 2022, "Harnessing the Multistability of Kresling Origami for Reconfigurable Articulation in Soft Robotic Arms," Soft Rob., 9(2), pp. 212–223.
- [152] Mukhopadhyay, T., Ma, J., Feng, H., Hou, D., Gattas, J. M., Chen, Y., and You, Z., 2020, "Programmable Stiffness and Shape Modulation in Origami Materials: Emergence of a Distant Actuation Feature," Appl. Mater. Today, 19, p. 100537.
- [153] Pagano, A., Yan, T., Chien, B., Wissa, A., and Tawfick, S., 2017, "A Crawling Robot Driven by Multi-Stable Origami," Smart Mater. Struct., 26(9), p. 094007
- [154] Cai, J., Deng, X., Zhang, Y., Feng, J., and Zhou, Y., 2016, "Folding Behavior of a Foldable Prismatic Mast With Kresling Origami Pattern," ASME J. Mech. Rob., 8, p. 031004.
- [155] Greco, M., Gesualdo, F. A. R., Venturini, W. S., and Coda, H. B., 2006, 'Nonlinear Positional Formulation for Space Truss Analysis," Finite Elem. Anal. Des., 42(12), pp. 1079–1086.
- [156] Kidambi, N., and Wang, K. W., 2020, "Dynamics of Kresling Origami Deployment," Phys. Rev. E, 101(6), p. 063003.
- [157] Fuchi, K., Buskohl, P. R., Bazzan, G., Durstock, M. F., Reich, G. W., Vaia, R. A., and Joo, J. J., 2015, "Origami Actuator Design and Networking Through Crease Topology Optimization," ASME J. Mech. Des., 137(9), p. 091401.
- [158] Zhu, Y., and Filipov, E., 2019, "An Efficient Numerical Approach for Simulating Contact in Origami Assemblages," Proc. R. Soc. A, 475(2230), p. 20190366.
- [159] Xia, Y., Filipov, E., and Wang, K. W., 2021, "The Deployment Dynamics and Multistability of Tubular Fluidic Origami," Active and Passive Smart Structures and Integrated Systems XV, J.-H. Han, G. Wang, and S. Shahab, eds., Vol. 11588, Online, Mar. 22, International Society for Optics and Photonics, pp. 98-108.
- [160] Xia, Y., Kidambi, N., Filipov, E. T., and Wang, K. W., 2022, "Deployment Dynamics of Miura Origami Sheets," ASME J. Comput. Nonlinear Dyn., 17(7), p. 071005.
- [161] Yu, Y., Chen, Y., and Paulino, G. H., 2019, "On the Unfolding Process of Triangular Resch Patterns: A Finite Particle Method Investigation," ASME Paper No. DETC2019-98121.
- [162] Xia, Y., and Wang, K.-W., 2019, "Dynamics Analysis of the Deployment of Miura-Origami Sheets," ASME Paper No. DETC2019-97136.
- [163] Dong, S., Zhao, X., and Yu, Y., 2021, "Dynamic Unfolding Process of Origami Tessellations," Int. J. Solids Struct., 226-227, p. 111075
- [164] Dong, S., and Yu, Y., 2021, "Numerical and Experimental Studies on Capturing Behaviors of the Inflatable Manipulator Inspired by Fluidic Origami
- Structures," Eng. Struct., 245, p. 112840.
  [165] Bhovad, P., and Li, S., 2021, "Physical Reservoir Computing With Origami and Its Application to Robotic Crawling," Sci. Rep., 11(1), p. 13002.
- [166] Zhang, H., 2021, "Mechanics Analysis of Functional Origamis Applicable in Biomedical Robots," IEEE/ASME Trans. Mechtronics, pp. 1-11.
- Zhang, H., Feng, H., Huang, J.-L., and Paik, J., 2021, "Generalized Modeling of Origami Folding Joints," Extreme Mech. Lett., 45, p. 101213.
- [168] Hu, Y. C., Zhou, Y. X., Kwok, K. W., and Sze, K. Y., 2021, "Simulating Flexible Origami Structures by Finite Element Method," Int. J. Mech. Mater. Des., 17(4), pp. 801-829.
- [169] Soleimani, H., Goudarzi, T., and Aghdam, M. M., 2021, "Advanced Structural Modeling of a Fold in Origami/Kirgami Inspired Structures," Thin-Walled Struct., 161, p. 107406.
- [170] Filipov, E. T., Paulino, G. H., and Tachi, T., 2016, "Origami Tubes With Reconfigurable Polygonal Cross-Sections," Proc. R. Soc. A, 472(2185), p. 20150607.
- [171] Grey, S. W., Scarpa, F., and Schenk, M., 2019, "Strain Reversal in Actuated Origami Structures," Phys. Rev. Lett., 123(2), p. 025501.
- [172] Cai, J., Ren, Z., Ding, Y., Deng, X., Xu, Y., and Feng, J., 2017, "Deployment Simulation of Foldable Origami Membrane Structures," Aerosp. Sci. Technol., 67, pp. 343-353.
- [173] Liu, S., Lu, G., Chen, Y., and Leong, Y. W., 2015, "Deformation of the Miura-Ori Patterned Sheet," Int. J. Mech. Sci., 99, pp. 130–142.
  [174] Ma, J., Hou, D., Chen, Y., and You, Z., 2018, "Peak Stress Relief of Cross
- Folding Origami," Thin-Walled Struct., 123, pp. 155–161.
- [175] Thai, P. T., Savchenko, M., and Hagiwara, I., 2018, "Finite Element Simulation of Robotic Origami Folding," Simul. Modell. Pract. Theory, 84, pp.
- [176] Yuan, L., Dai, H., Song, J., Ma, J., and Chen, Y., 2020, "The Behavior of a Functionally Graded Origami Structure Subjected to Quasi-Static Compression," Mater. Des., 189, p. 108494.
- [177] Karagiozova, D., Zhang, J., Lu, G., and You, Z., 2019, "Dynamic Inplane Compression of Miura-Ori Patterned Metamaterials," Int. J. Impact Eng., 129, pp. 80-100.
- [178] Zhang, J., Karagiozova, D., You, Z., Chen, Y., and Lu, G., 2019, "Quasi-Static Large Deformation Compressive Behaviour of Origami-Based Metamaterials," Int. J. Mech. Sci., 153-154, pp. 194-207.
- [179] Schenk, M., Guest, S. D., and McShane, G. J., 2014, "Novel Stacked Folded Cores for Blast-Resistant Sandwich Beams," Int. J. Solids Struct., 51(25-26), pp. 4196-5214.
- [180] Heimbs, S., Middendorf, P., Kilchert, S., Johnson, A. F., and Maier, M., 2007, "Experimental and Numerical Analysis of Composite Folded Sandwich Core Structures Under Compression," Appl. Compos. Mater., 14(5–6), pp. 363–377.
- [181] Heimbs, S., Cichosz, J., Klaus, M., Kilchert, S., and Johnson, A. F., 2010, "Sandwich Structures With Textile-Reinforced Composite Foldcores Under Impact Loads," Compos. Struct., 92(6), pp. 1485-1497.

- [182] Xiang, X., Lu, G., and You, Z., 2020, "Energy Absorption of Origami Inspired
- Structures and Materials," Thin-Walled Struct., 157, p. 107130. [183] Ma, J., and You, Z., 2014, "Energy Absorption of Thin-Walled Square Tubes With a Prefolded Origami Pattern-Part 1: Geometry and Numerical Simulation," ASME J. Appl. Mech., 81(1), p. 011003.
- [184] Wang, B., and Zhou, C., 2017, "The Imperfection-Sensitivity of Origami
- Crash Boxes," Int. J. Mech. Sci., 121, pp. 58–66.

  [185] Song, J., Chen, Y., and Lu, G., 2012, "Axial Crushing of Thin-Walled Structures With Origami Patterns," Thin-Walled Struct., 54, pp. 65–71.
- [186] Yang, K., Xu, S., Shen, J., Zhou, S., and Xie, Y. M., 2016, "Energy Absorption of Thin-Walled Tubes With Pre Folded Origami Patterns: Numerical Simulation and Experimental Verification," Thin-Walled Struct., 103, pp. 33-44.
- [187] Zaghloul, A., and Bone, G. M., 2020, "3D Shrinking for Rapid Fabrication of Origami-Inspired Semi-Soft Pneumatic Actuators," IEEE Access, 8, pp. 191330-191340.
- [188] Xiang, X., You, Z., and Lu, G., 2018, "Rectangular Sandwich Plates With Miura-Ori Folded Core Under Quasi-Static Loadings," Compos. Struct., 195,
- [189] Peraza Hernandez, E. A., Hartl, D. J., Malak, R. J., Akleman, E., Gonen, O., and Kung, H.-W., 2016, "Design Tools for Patterned Self-Folding Reconfigurable Structures Based on Programmable Active Laminates," ASME J. Mech. Rob., 8(3), p. 031015.
- [190] Kwok, T.-H., 2021, "Geometry-Based Thick Origami Simulation," ASME J. Mech. Des., 143(6), p. 061701.
- [191] McGuire, W., Gallagher, R. H., and Ziemian, R. D., 2000, Matrix Structural Analysis, 2nd ed., Createspace Independent Publishing Platform, Scotts Valley, CA.
- [192] Liu, K., and Paulino, G., 2016, "MERLIN: A MATLAB Implementation to Capture Highly Nonlinear Behavior of Non-Rigid Origami," Proceedings of IASS Annual Symposium, Tokyo, Japan, Sept. 26-30, International Associa-
- tion for Shell and Spatial Structures, pp. 1–10. [193] Liu, K., and Paulino, G., 2018, "Highly Efficient Structural Analysis of Origami Assemblages Using the merlin2 Software," Origami 7, Seventh International Meeting on Origami in Science, Mathematics and Education (70SME), Oxford University, Oxford, UK, Sept. 5-7.
- [194] Redoutey, M., Roy, A., and Filipov, E. T., 2021, "Pop-Up Kirigami for Stiff, Dome-Like Structures," Int. J. Solids Struct., 229, p. 111140.
- [195] Ghassaei, A., Demaine, E. D., and Gershenfeld, N., 2018, "Fast, Interactive Origami Simulation Using GPU Computation," Proceedings of the Seventh International Meeting on Origami in Science, Mathematics and Education, Fast, Interactive Origami Simulation Using GPU Computation Vol. 4, Oxford, UK, Sept. 5-7, pp. 1151-1166.
- [196] Masana, R., and Daqaq, M. F., 2019, "Equilibria and Bifurcations of a Foldable Paper-Based Spring Inspired by Kresling-Pattern Origami," Phys. Rev. E, 100(6), p. 063001.
- [197] Pratapa, P. P., Liu, K., Vasudevan, S. P., and Paulino, G. H., 2021, "Reprogrammable Kinematic Branches in Tessellated Origami Structures," ASME J. Mech. Rob., **13**(3), p. 031102.
- [198] Yu, Y., Paulino, G. H., and Luo, Y., 2011, "Finite Particle Method for Progressive Failure Simulation of Truss Structures," J. Struct. Eng., 137(10), pp. 1168-1181.
- [199] Fonseca, L. M., Rodrigues, G. V., Savi, M. A., and Paiva, A., 2019, "Nonlinear Dynamics of an Origami Wheel With Shape Memory Alloy Actuators," Chaos, Solitons Fractals, 122, pp. 245-261.
- [200] Yasuda, H., Yamaguchi, K., Miyazawa, Y., Wiebe, R., Raney, J. R., and Yang, J., 2020, "Data-Driven Prediction and Analysis of Chaotic Origami Dynamics," Commun. Phys., 3(1), p. 168.
- [201] Han, H., Tang, L., Cao, D., and Liu, L., 2020, "Modeling and Analysis of Dynamic Characteristics of Multi-Stable Waterbomb Origami Base," Nonlinear Dyn., 102(4), pp. 2339–2362.
- [202] Kwok, T.-H., Wang, C. C. L., Deng, D., Zhang, Y., and Chen, Y., 2015, "Four-Dimensional Printing for Freeform Surfaces: Design Optimization of
- Origami and Kirigami Structures," J. Mech. Des., 137(11), p. 111413.

  [203] Faber, J., Arrieta, A. F., and Studart, A. R., 2018, "Bioinspired Spring Origami," Science, 359(6382), pp. 1386–1391.

  [204] Liu, K., and Paulino, G. H., 2017, "MERLIN," Princeton University, Prince-
- ton, NJ, accessed Dec. 2021, http://paulino.princeton.edu/software.html
- [205] Zhu, Y., and Filipov, E. T., 2021, "Sequentially Working Origami Multi-Physics Simulator (SWOMPS)," University of Michigan, Ann Arbor, MI, accessed Dec. 2021, https://github.com/zzhuyii/OrigamiSimulator
- [206] Ma, J., Hou, D., Chen, Y., and You, Z., 2016, "Quasi-Static Axial Crushing of the Thin-Walled Tubes With a Kite-Shape Rigid Origami Pattern: Numerical Simulation," Thin-Walled Struct., 100, pp. 38–47. [207] MIT, 2017, "About Contact Interactions," MIT, Cambridge, MA, accessed
- Dec. 2021, https://abaqus-docs.mit.edu/2017/English/SIMACAEITNRefMap/ imaitn-c-contactoverview.htm
- [208] MIT, 2017, "Common Difficulties Associated With Contact Modeling in Abaqus/Standard," MIT, Cambridge, MA, accessed Dec. 2021, http:// 194.167.201.93/English/SIMACAEITNRefMap/simaitn-c-contacttrouble.htm
- [209] MIT, 2017, "Common Difficulties Associated With Contact Modeling Using Contact Pairs in Abaqus/Explicit," MIT, Cambridge, MA, accessed Dec. 2021, https://abaqus-docs.mit.edu/2017/English/SIMACAEITNRefMap/ simaitn-c-expcontacttrouble.htm
- [210] Swaminathan, R., Cai, C. J., Yuan, S., and Ren, H., 2021, "Multiphysics Simulation of Magnetically Actuated Robotic Origami Worms," IEEE Rob. Autom. Lett., **6**(3), pp. 4923–4930.

- [211] Leong, T. G., Randall, C. L., Benson, B. R., Zarafshar, A. M., and Gracias, D. H., 2008, "Self-Loading Lithographically Structured Microcontainers: 3D Patterned, Mobile Microwells," Lab Chip, 8(10), pp. 1621-1624.
- [212] Arora, W. J., Nichol, A. J., Smith, H. I., and Barbastathis, G., 2006, "Membrane Folding to Achieve Three-Dimensional Nanostructures: Nanopatterned Silicon Nitride Folded With Stressed Chromium Hinges," Appl. Phys. Lett., 88(5), p. 053108.
- [213] Paik, J. K., and Wood, R. J., 2012, "A Bidirectional Shape Memory Alloy Folding Actuator," Smart Mater. Struct., 21(6), p. 065013.
- [214] Shaar, N. S., Barbastathis, G., and Livermore, C., 2015, "Integrated Folding, Alignment, and Latching for Reconfigurable Origami Microelectromechanical Systems," J. Microelectromech. Syst., 24(4), pp. 1043–1051.
  [215] Iwase, E., and Shimoyama, I., 2005, "Multistep Sequential Batch Assembly of
- Three-Dimensional Ferromagnetic Microstructures With Elastic Hinges," J. Microelectromech. Syst., 14(6), pp. 1265–1271.
- [216] Xu, T., Zhang, J., Salehizadeh, M., Onaizah, O., and Diller, E., 2019, "Millimeter-Scale Flexible Robots With Programmable Three-Dimensional Magnetization and Motions," Sci. Rob., 4(29), p. eaav4494.
- [217] Timoshenko, S., 1925, "Analysis of Bi-Metal Thermostats," J. Opt. Soc. Am., 11, pp. 233-255.
- [218] Deng, D., Yang, Y., Chen, Y., Lan, X., and Tice, J., 2017, "Accurately Controlled Sequential Self-Folding Structures by Polystyrene Film," Smart Mater. Struct., 26(8), p. 085040.
- [219] Piker, D., 2017, "Kangaroo," KANGAROO PHYSICS, Barcelona, Spain, accessed Dec. 2021, https://www.food4rhino.com/en/app/kangaroo-physic
- [220] Piker, D., 2013, "Kangaroo: Form Finding With Computational Physics," Archit. Des., 83(2), pp. 136–137.
- [221] Chen, T., Bilal, O. R., Lang, R., Daraio, C., and Shea, K., 2019, "Autonomous Deployment of a Solar Panel Using Elastic Origami and Distributed Shape-Memory-Polymer Actuators," Phys. Rev. Appl., 11(6), p. 064069.
- [222] Fuchi, K., Tang, J., Crowgey, B., Diaz, A. R., Rothwell, E. J., and Ouedraogo, R. O., 2012, "Origami Tunable Frequency Selective Surfaces," IEEE Antennas Wireless Propagation Lett., 11, pp. 473–475.
- [223] Fuchi, K., Buskohl, P. R., Bazzan, G., Durstock, M. F., Joo, J. J., Reich, G. W., and Vaia, R. A., 2016, "Spatial Tuning of a RF Frequency Selective Surface Through Origami," Automatic Target Recognition XXVI, F. A. Sadjadi, and A. Mahalanobis, eds., Vol. 9844, Baltimore, MD, May 12, SPIE, pp.
- [224] Cui, Y., Nauroze, S. A., and Tentzeris, M. M., 2019, "Novel 3D-Printed Reconfigurable Origami Frequency Selective Surfaces With Flexible Inkjket-Printed Conductor Traces," IEEE/MTT-S International Microwave Symposium, Vol. 11, Boston, MA, June 2-7, pp. 1367-1370.
- [225] Biswas, A., Zekios, C. L., and Georgakopoulos, S. V., 2020, "Transforming Single-Band Static FSS to Dual-Band Dynamic FSS Using Origami," Sci. Rep., 10(1), p. 13884.
- [226] Pratapa, P. P., Suryanarayana, P., and Paulino, G. H., 2018, "Bloch Wave Framework for Structures With Nonlocal Interactions: Application to the

- Design of Origami Acoustic Metamaterials," J. Mech. Phys. Solids, 118, pp. 115-132
- [227] Thota, M., and Wang, K., 2018, "Tunable Waveguiding in Origami Phononic Structures," J. Sound Vib., **430**, pp. 93–100. [228] Zhu, Y., Fei, F., Fan, S., Cao, L., Donda, K., and Assouar, B., 2019,
- "Reconfigurable Origami-Inspired Metamaterials for Controllable Sound Manipulation," Phys. Rev. Appl., 12(3), p. 034029.
- [229] Demaine, E., Ku, J., and Lang, R., 2021, "Fold," accessed Dec. 2021, https:// github.com/edemaine/fold
- [230] Tachi, T., 2009, "Rigid Origami Simulator," The University of Tokyo, Tokyo, Japan, accessed Dec. 2021, https://tsg.ne.jp/TT/software/index.html
  [231] Tachi, T., 2010, "Origamizer," The University of Tokyo, Tokyo, Japan,
- accessed Dec. 2021, https://tsg.ne.jp/TT/software/index.html [232] Ghassaei, A., 2017, "Origami Simulator," accessed Dec. 2021, https:// origamisimulator.org/
- [233] Fuchi, K., 2022, "Origami Mechanism Topology Optimizer (OMTO)," Air Force Research Laboratory, Dayton, OH, accessed Dec. 2021, https:// www.mathworks.com/matlabcentral/fileexchange/51811-origami-mechanismtopology-optimizer-omto
- [234] Gillman, A., 2018, "Origami Topology Optimization w/Nonlinear Truss Model," Air Force Research Laboratory, Dayton, OH, accessed Dec. 2021, https://www.mathworks.com/matlabcentral/fileexchange/69612-origami-topologyoptimization-w-nonlinear-truss-model
- [235] Suto, K., and Tanimichi, K., 2021, "Crane," Nature Architects Inc, JP, accessed Dec. 2021, https://www.food4rhino.com/en/app/crane
- [236] Novelino, L. S., Ze, Q., Wu, S., Paulino, G. H., and Zhao, R., 2020, "Untethered Control of Functional Origami Microrobots With Distributed
- Actuation," Proc. Natl. Acad. Sci., 117(39), pp. 24096–24101.

  [237] Hwang, H.-Y., 2021, "Effects of Perforated Crease Line Design on Mechanical Behaviors of Origami Structures," Int. J. Solids Struct., 230–231, p. 111158
- [238] Dudte, L. H., Vouga, E., Tachi, T., and Mahadevan, L., 2016, "Programming Curvature Using Origami Tessellations," Nat. Mater., 15(5), pp. 583-588.
- [239] Miyazawa, Y., Yasuda, H., Kim, H., Lynch, J. H., Tsujikawa, K., Kunimine, T., Raney, J. R., and Yang, J., 2021, "Heterogeneous Origami-Architected Materials With Variable Stiffness," Commun. Mater., 2(1), pp. 1-7.
- [240] Woo, A. C., Wang, H. T. G., Schuh, M. J., and Sanders, M. L., 1993, "EM Programmer's Notebook-Benchmark Radar Targets for the Validation of Computational Electromagnetics Programs," IEEE Antennas Propag. Mag., 35(1), pp. 84-89.
- [241] Pinson, M. B., Stern, M., Ferrero, A. C., Witten, T. A., Chen, E., and Murugan, A., 2017, "Self-Folding Origami at Any Energy Scale," Nat. Commun., 8(1),
- [242] Grey, S. W., Scarpa, F., and Schenk, M., 2020, "Mechanics of Paper-Folded Origami: A Cautionary Tale," Mech. Res. Commun., 107, p. 103540.